

Comprehensive two-dimensional gas chromatography coupled to high resolution time-of-flight mass spectrometry for screening of organohalogenated compounds in cat hair

Martin Brits ^{a,b,c}, Peter Gorst-Allman ^d, Egmont R. Rohwer ^c, Jayne De Vos ^a, Jacob de Boer ^b, Jana M. Weiss ^{ef}

^a National Metrology Institute of South Africa (NMISA), CSIR Campus, Meiring Naude Road, Pretoria 0040, South Africa

^b VU University, Department Environment and Health, De Boelelaan 1087, 1081 HV Amsterdam, The Netherlands

^c Laboratory for Separation Science, Department of Chemistry, Faculty of Natural and Agricultural Sciences, University of Pretoria, Lynnwood Road, Pretoria 0002, South Africa

^d LECO Africa, Kempton Park, South Africa

^e Department of Environmental Science and Analytical Chemistry, Arrhenius Laboratory, Stockholm University, SE-10691 Stockholm

^f Department of Aquatic Sciences and Assessment, Swedish University of Agricultural Sciences, SE-750 07 UPPSALA

Supporting Information:

- Detailed description of GCxGC–HR-TOFMS instrument parameters.
- Mass spectra comparison with commercial mass spectral database results

GCxGC–HR-TOFMS instrumental parameters:

The instrument control, data acquisition (100 Hz) and processing was carried out using Chroma-TOF software (LECO Corporation, St Joseph, MI, USA). The GCxGC separation was achieved using a 15 m Rxi-5HT (0.25 mm I.D. × 0.1 µm df; Restek, Bellefonte, USA) as the first dimension (1D) column and 1 m Rxi-PAH (0.25 mm I.D. × 0.1 µm df; Restek, Bellefonte, USA) as the second dimension column. The injector and transfer line temperatures were maintained at 280 °C and 320 °C, respectively. The ion source temperatures was set at 250 °C and operated at 70 eV. Helium (99.999%; Air Products, Kempton Park, South Africa) was used as the carrier gas at 1.0 mL/ min. Injections of 1 µL aliquots were made in the splitless mode with a 60 s purge delay and the primary GC oven temperature was

kept constant at 90 °C for 1 min, raised at 10 °C per minute to 320 °C, and held for 5 min. The secondary oven temperature was programmed as the primary oven with a +20 °C offset. The modulation period was set to 6 s with a 1.8 s hot pulse and the modulator temperature was programmed as the primary oven with a +15 °C offset relative to the secondary oven temperature. During modulation, cold pulses were generated using dry nitrogen gas cooled by liquid nitrogen (Air Products, Kempton Park, South Africa), and hot pulses through dry nitrogen heated by a modulator heating block. Modulation gasses were supplied from a nitrogen generator (Genius 1052, Peak Scientific, Scotland). Full scan data was collected at an acquisition rate of 60 spectra/ s and extraction frequency of 1.4 kHz in the high resolution mode (>25,000 FWHM at m/z 218.98).

Mass spectra comparison with commercial mass spectral database results

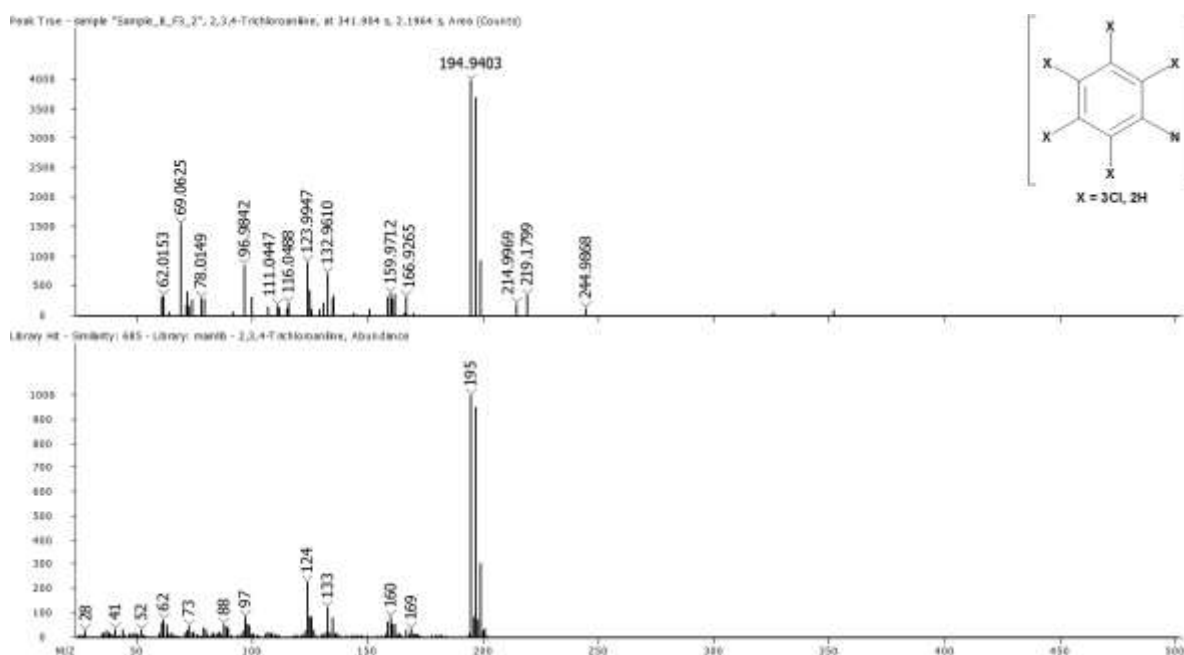


Fig. S1. Trichloroaniline

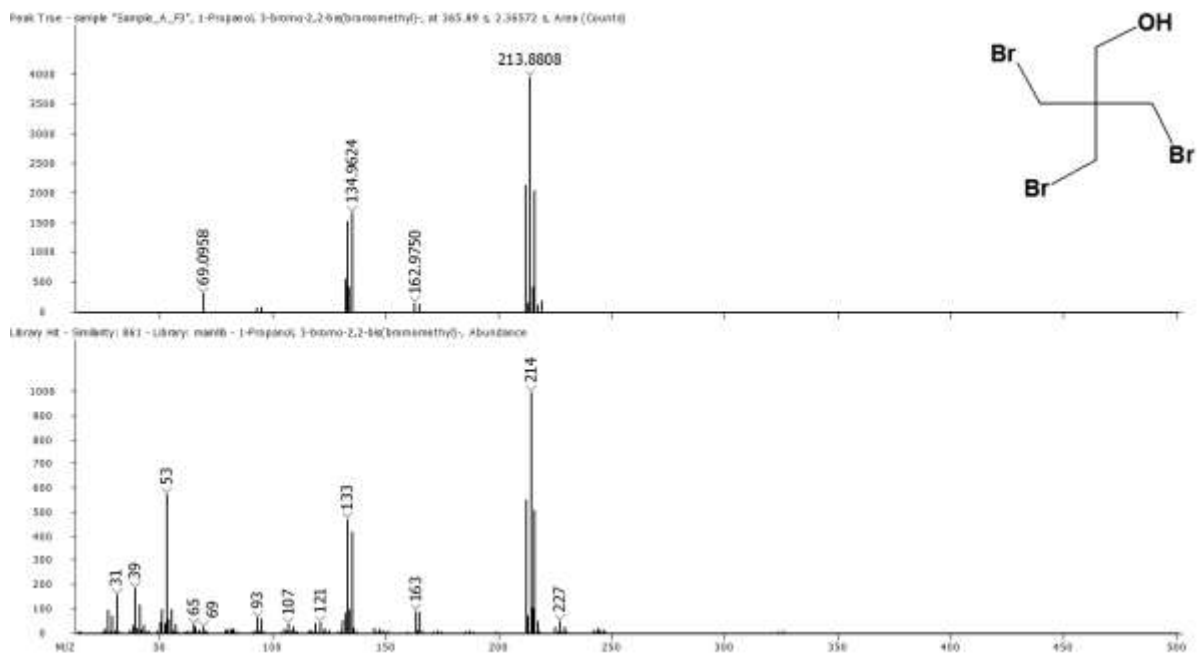


Fig. S2. Trisbromoneopentyl alcohol (TBNPA)

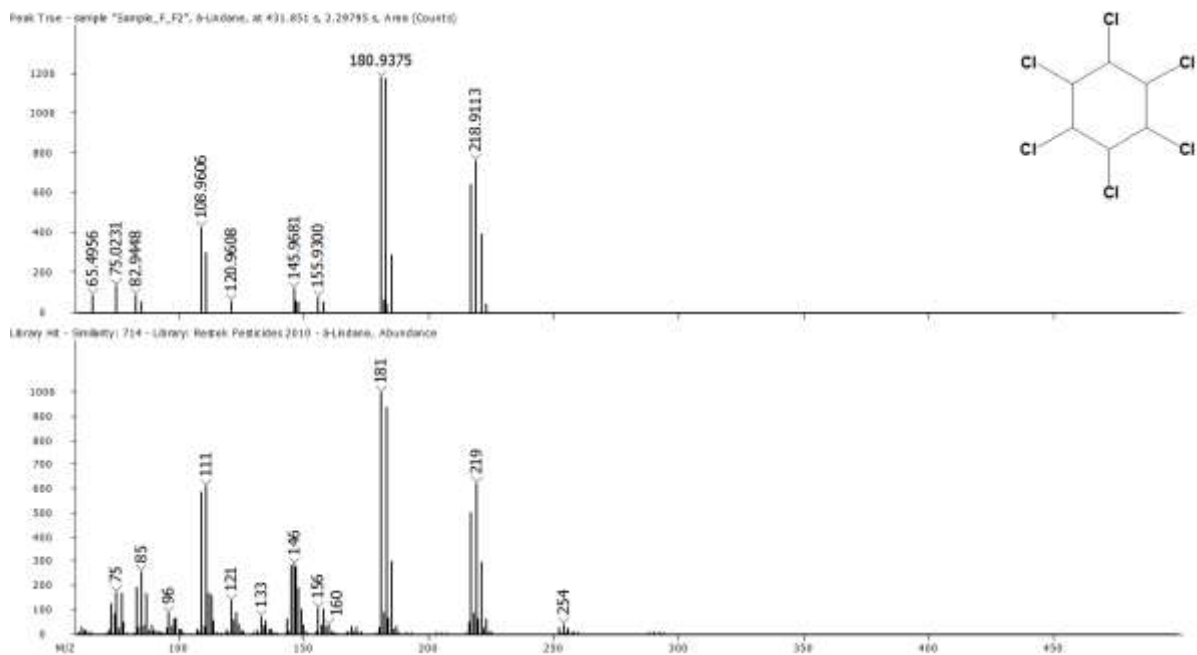


Fig. S3. Alpha-hexachlorocyclohexane

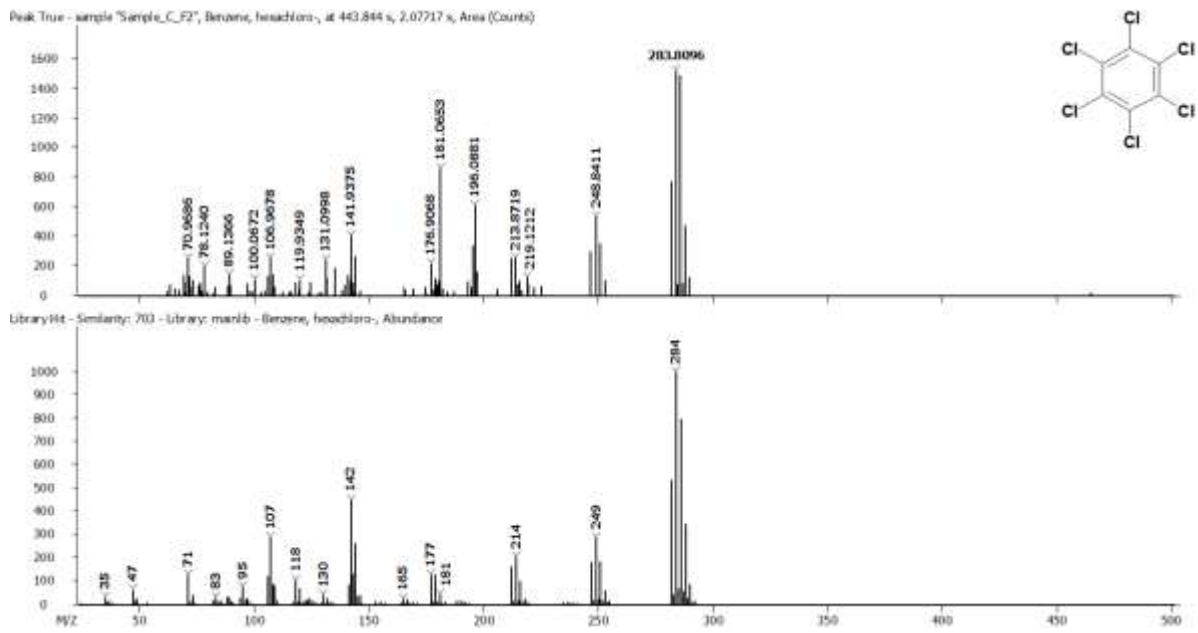


Fig. S4. Hexachlorobenzene (HCB)

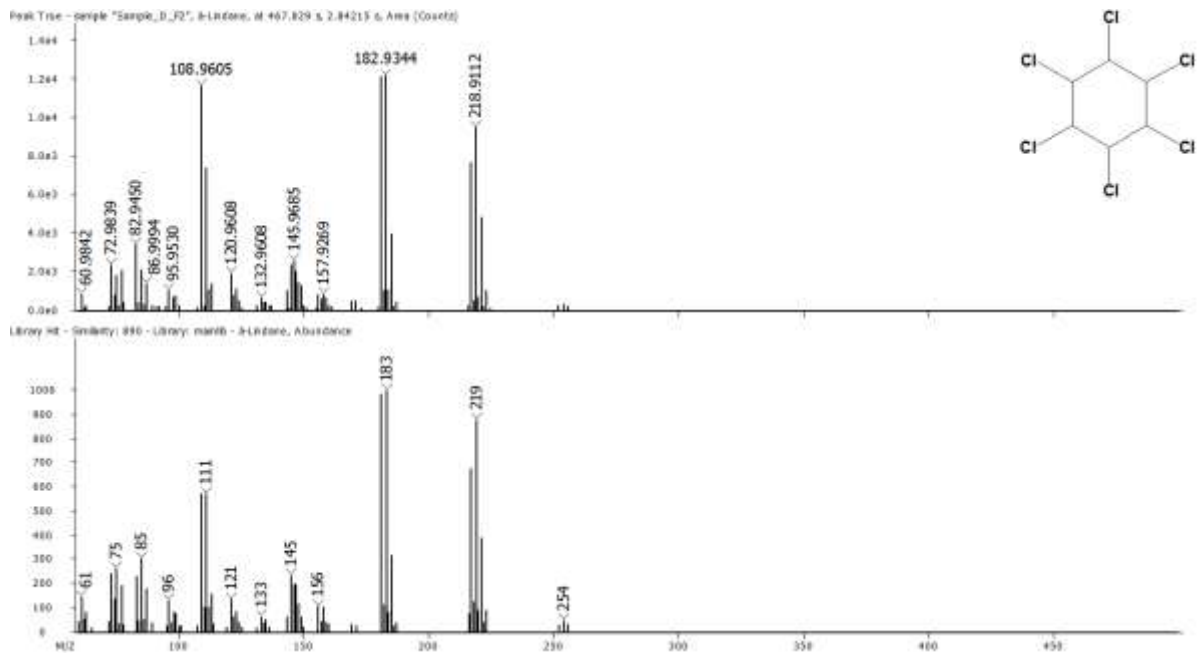


Fig. S5. Beta-hexachlorocyclohexane

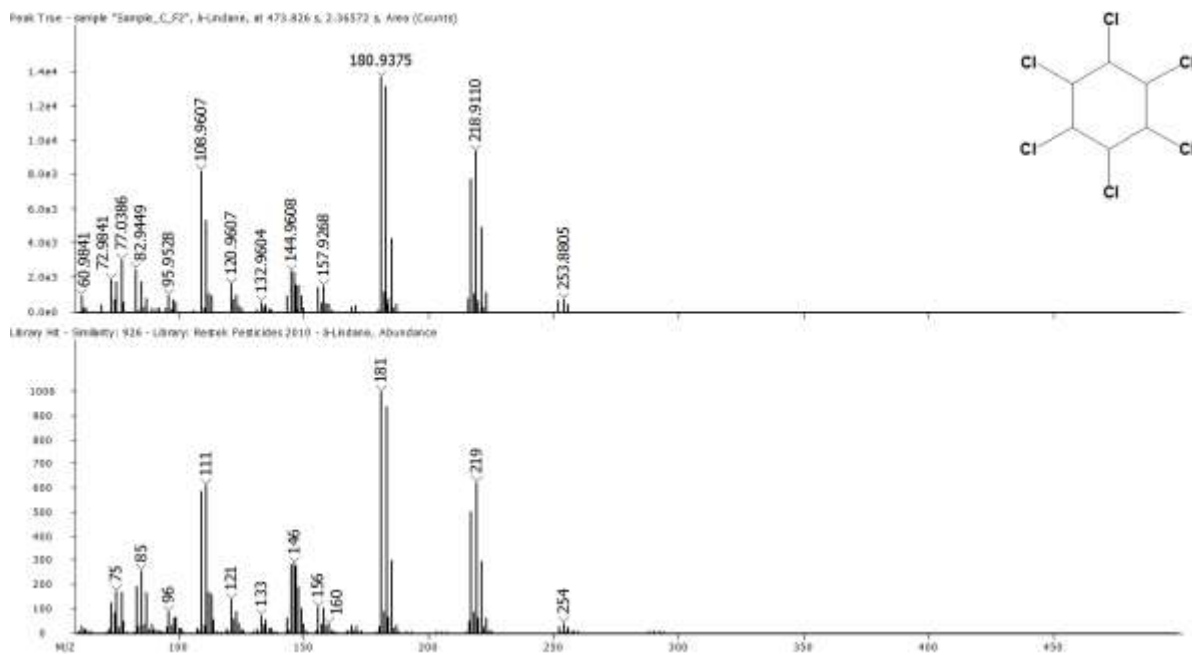


Fig. S6. Gamma-hexachlorocyclohexane

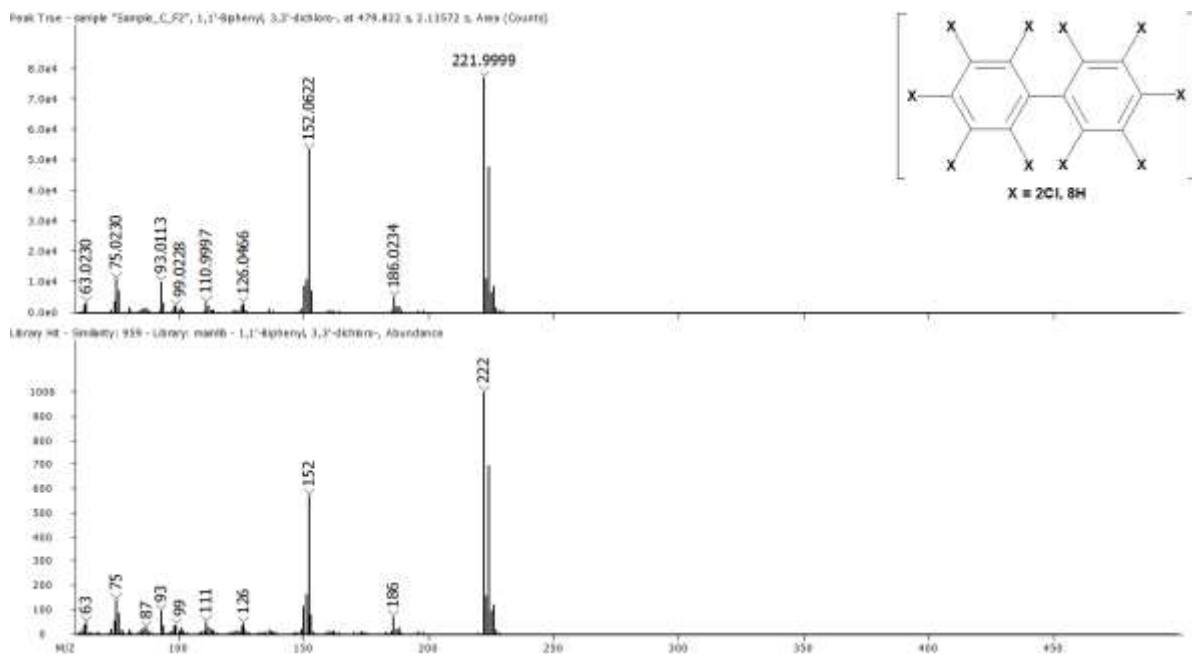


Fig. S7. Dichlorobiphenyl (Di-CB)

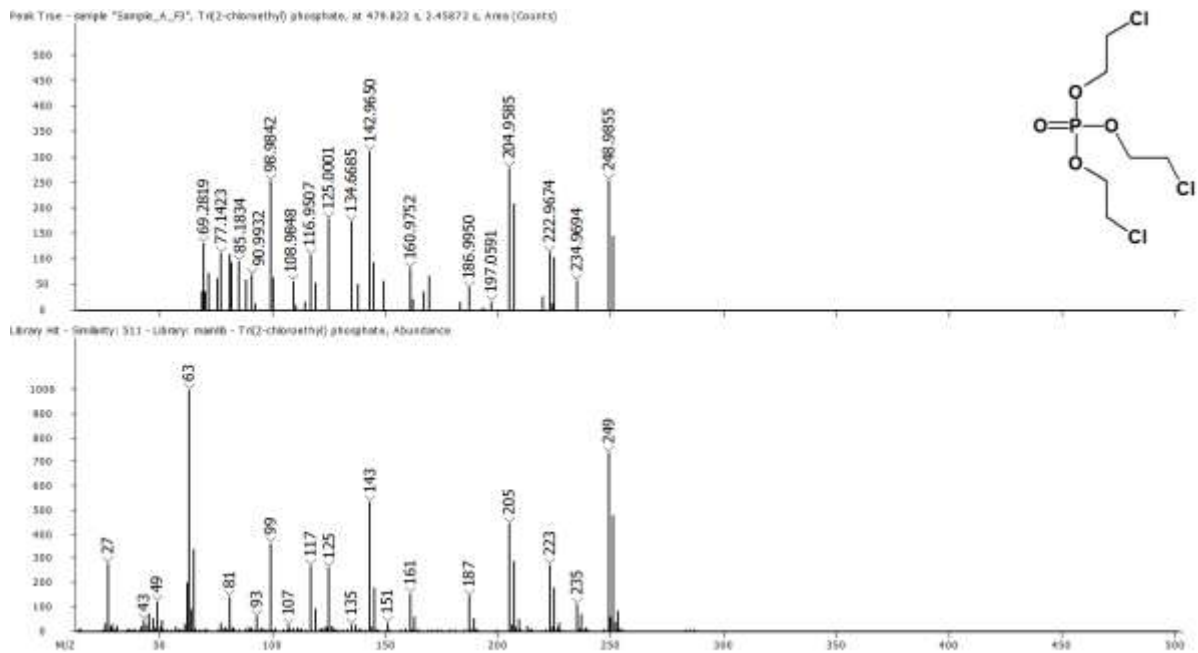


Fig. S8. Tri(2-chloroethyl) phosphate (TCEP)

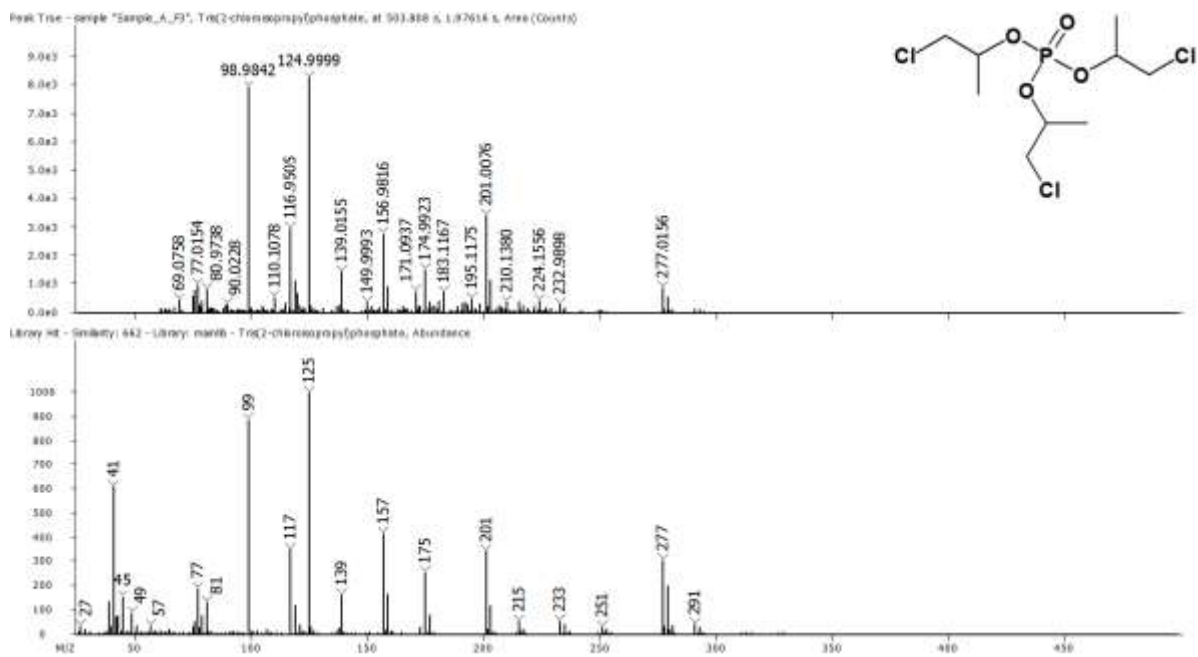


Fig. S9. Tris(2-chloroisopropyl)phosphate (TCIPP)

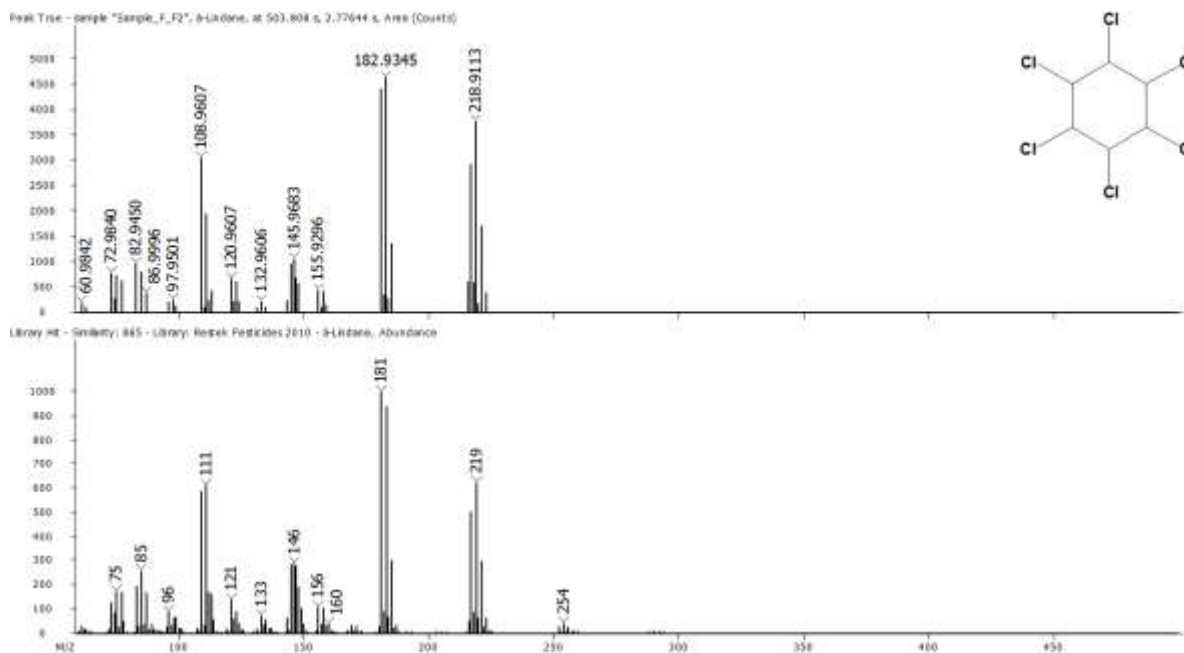


Fig. S10. Delta-hexachlorocyclohexane

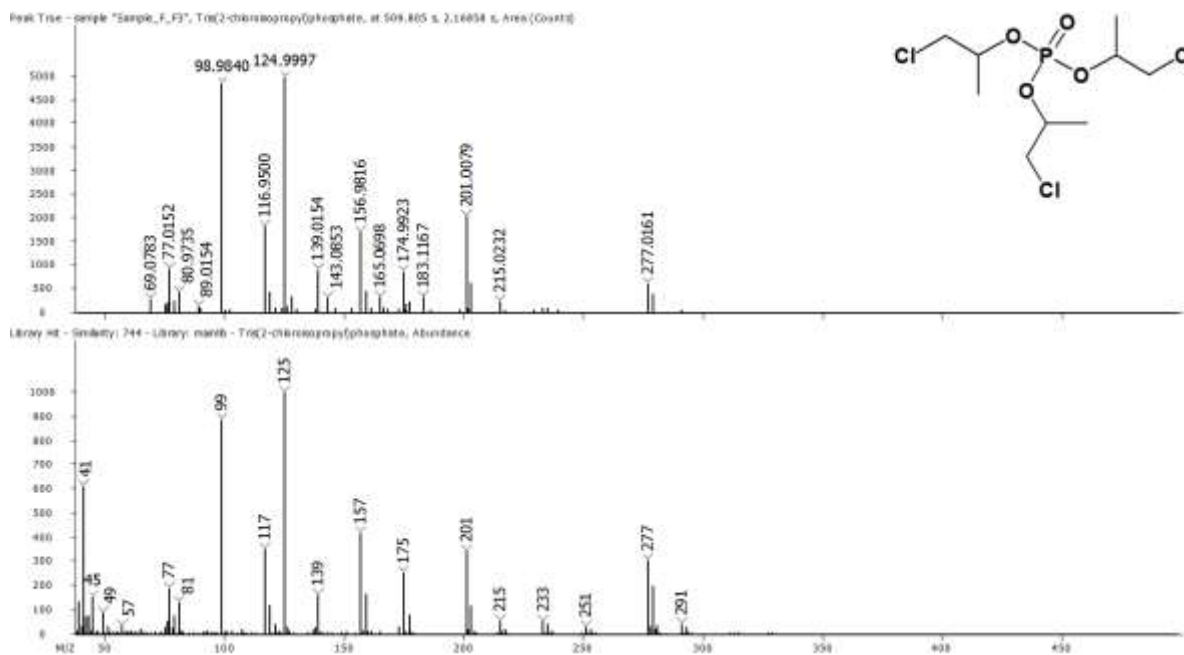


Fig. S11. Tris(2-chloroisopropyl)phosphate (TCIPP)

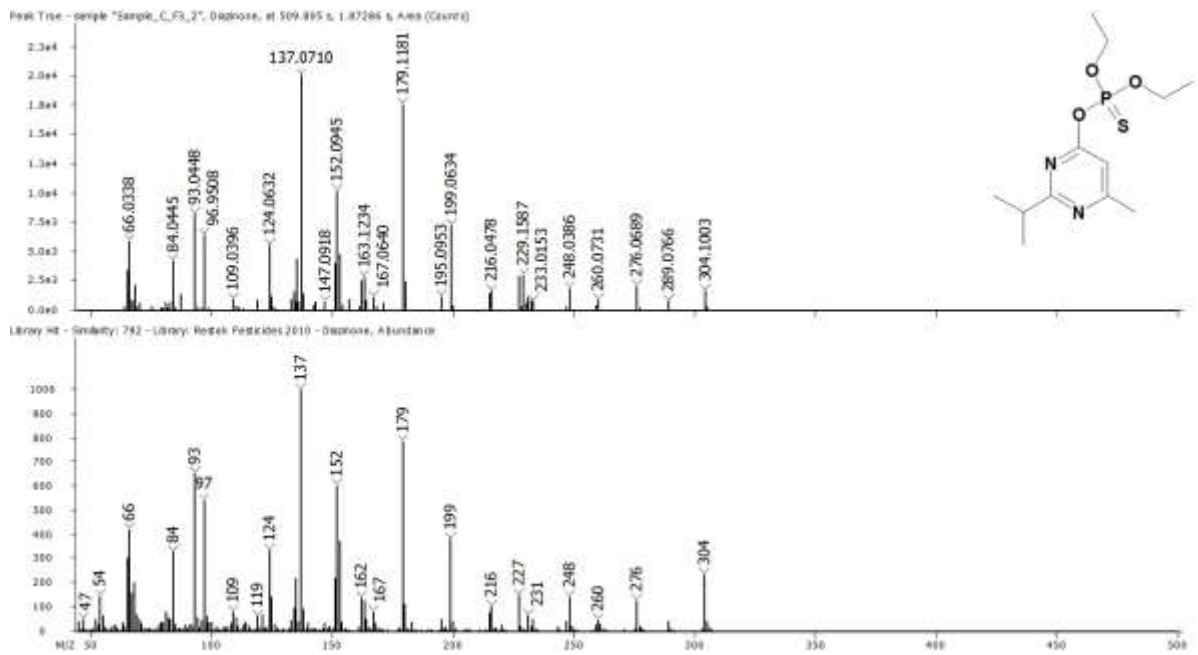


Fig. S12. Diazinone

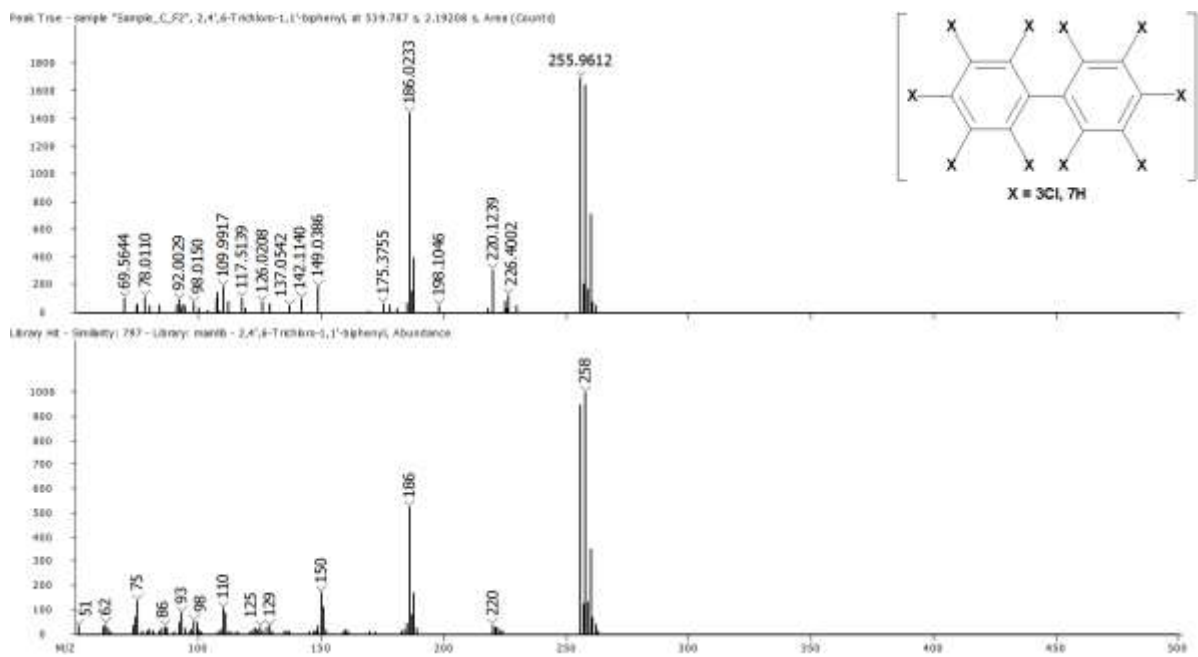


Fig. S13. Trichlorobiphenyls (Tri-CB)

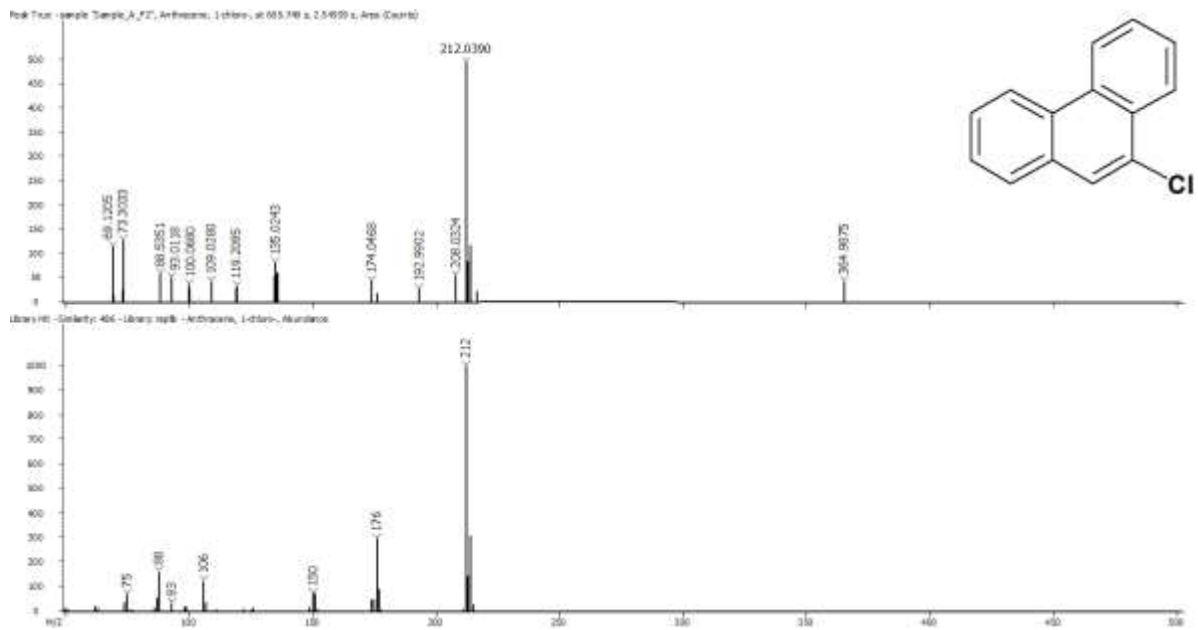


Fig. S14. Dichloroanthracene

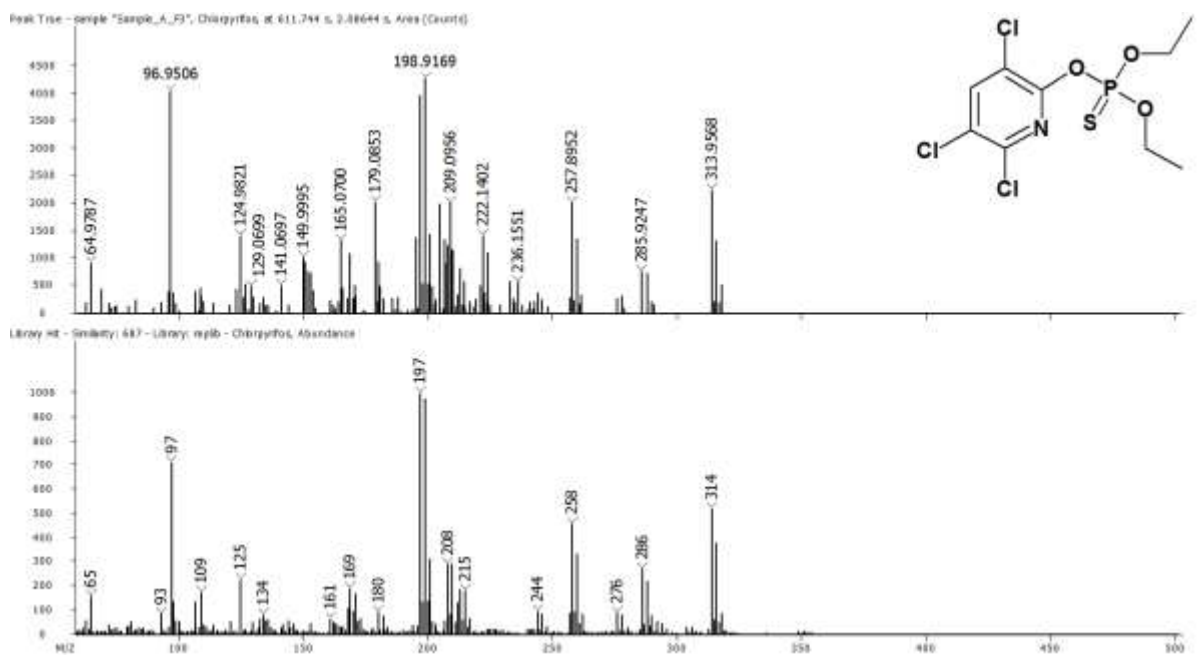


Fig. S15. Chlorpyrifos

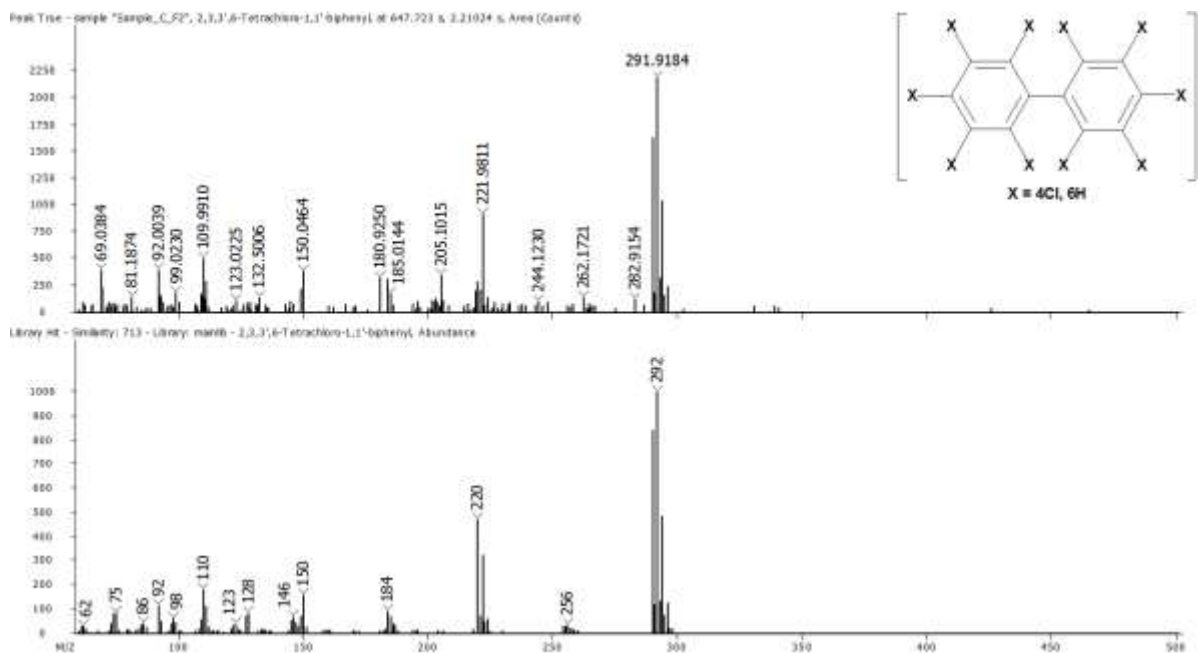


Fig. S16. Tetrachlorobiphenyls (Tetra-CB)

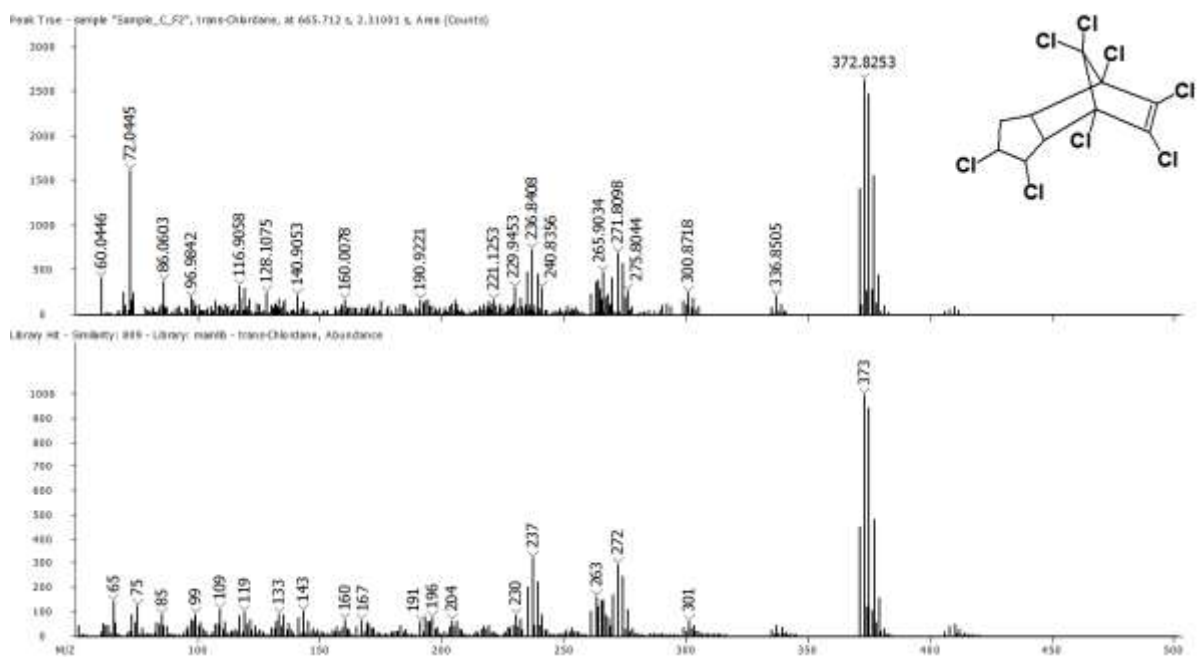


Fig. S17. trans-Chlordane

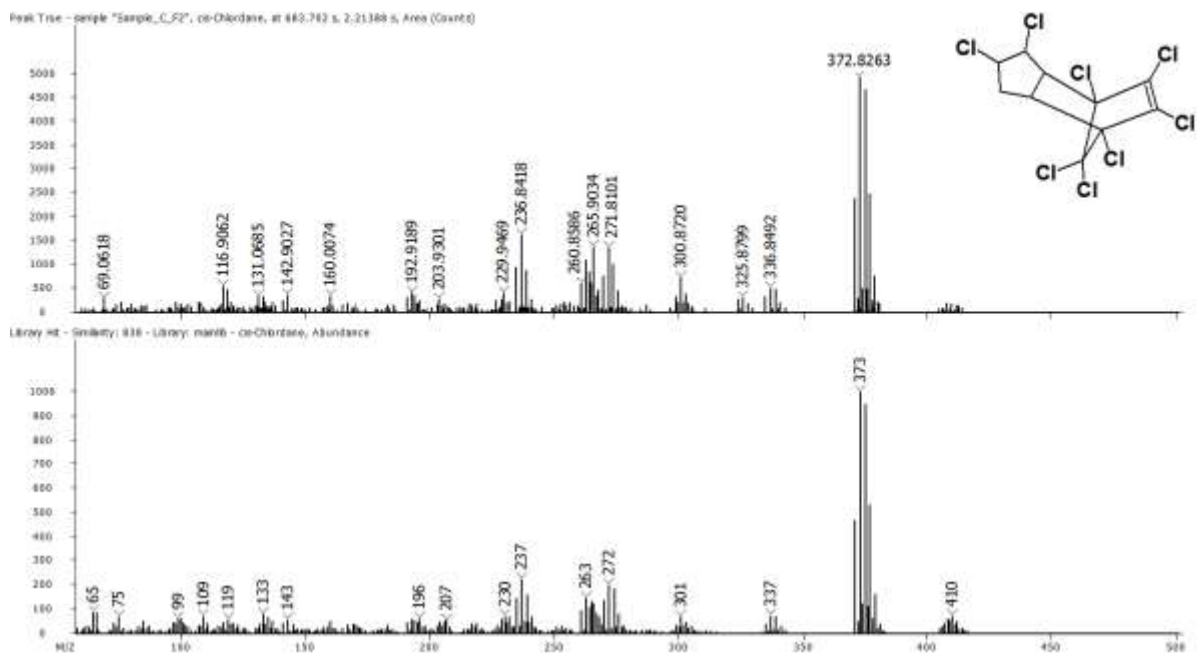


Fig. S18. cis-Chlordane

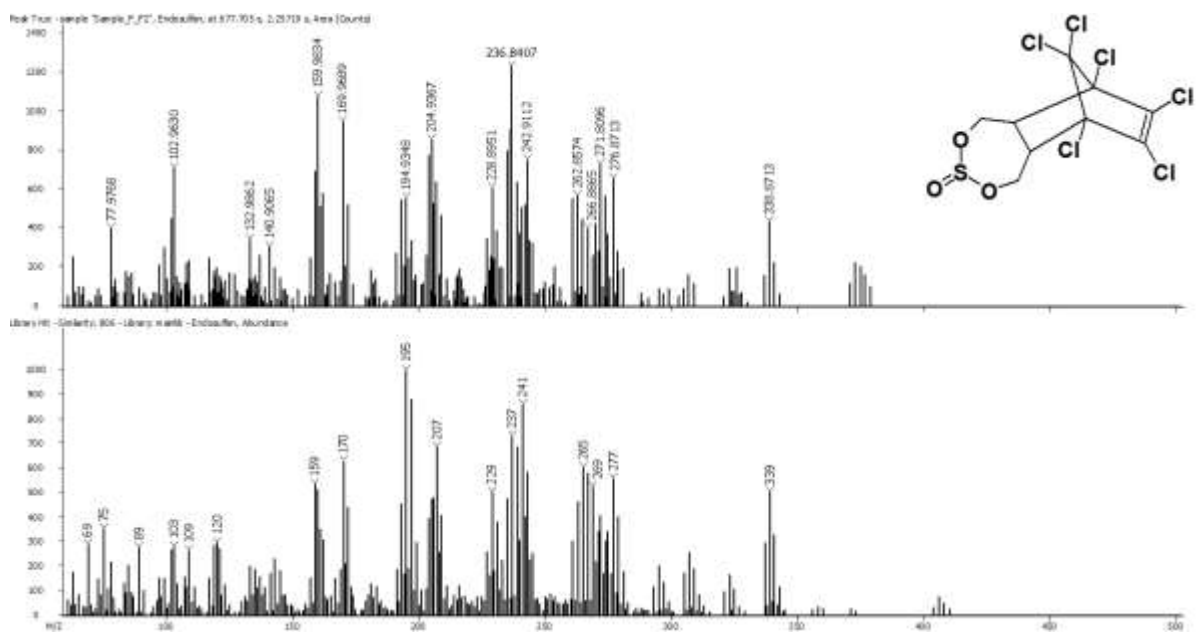


Fig. S19. Endosulfan I

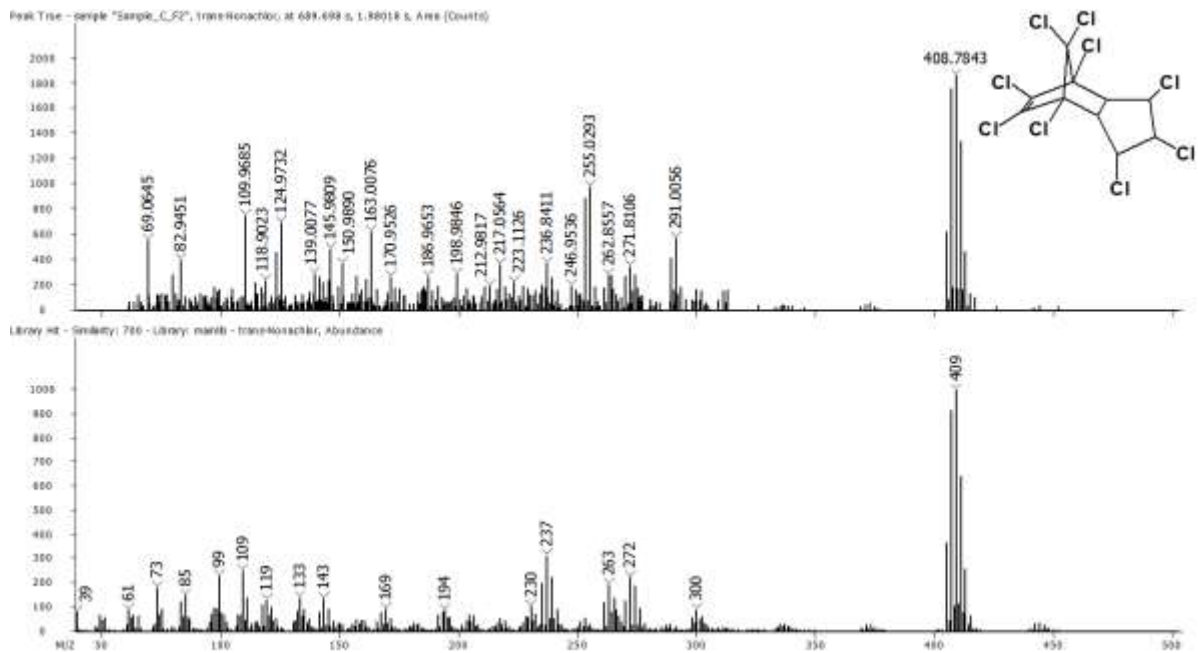


Fig. S20. trans-Nonachlor

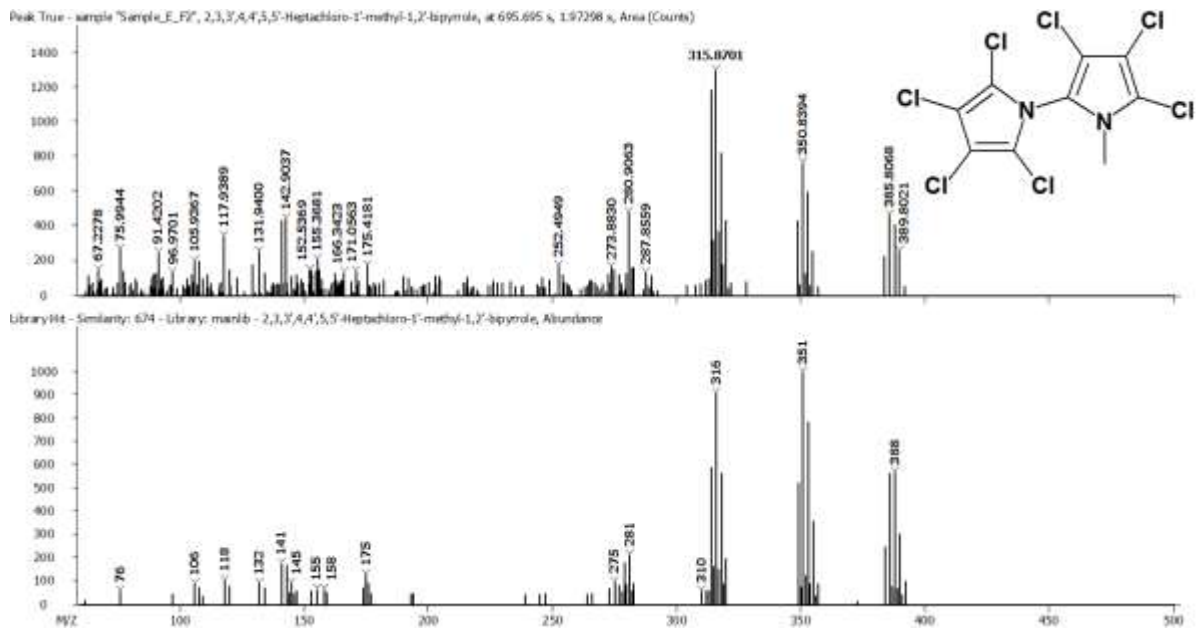


Fig. S21. 2,3,3',4,4',5,5'-Heptachloro-1'-methyl-1,2'-bipyrrrole

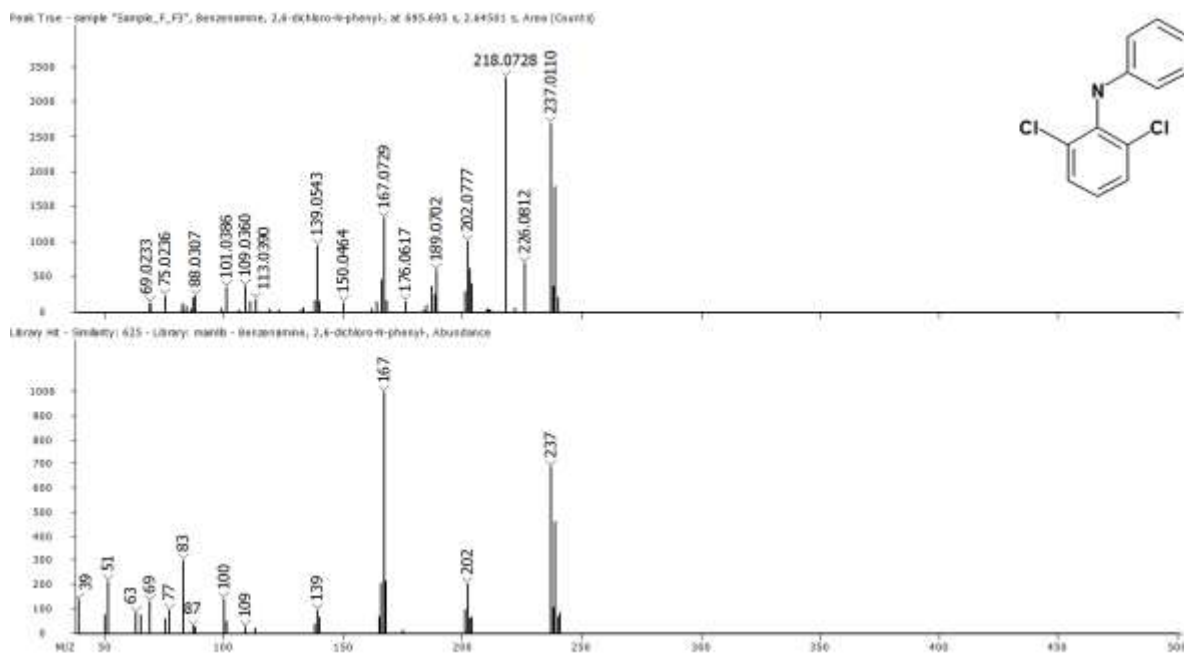


Fig. S22. Dichlorophenylaniline

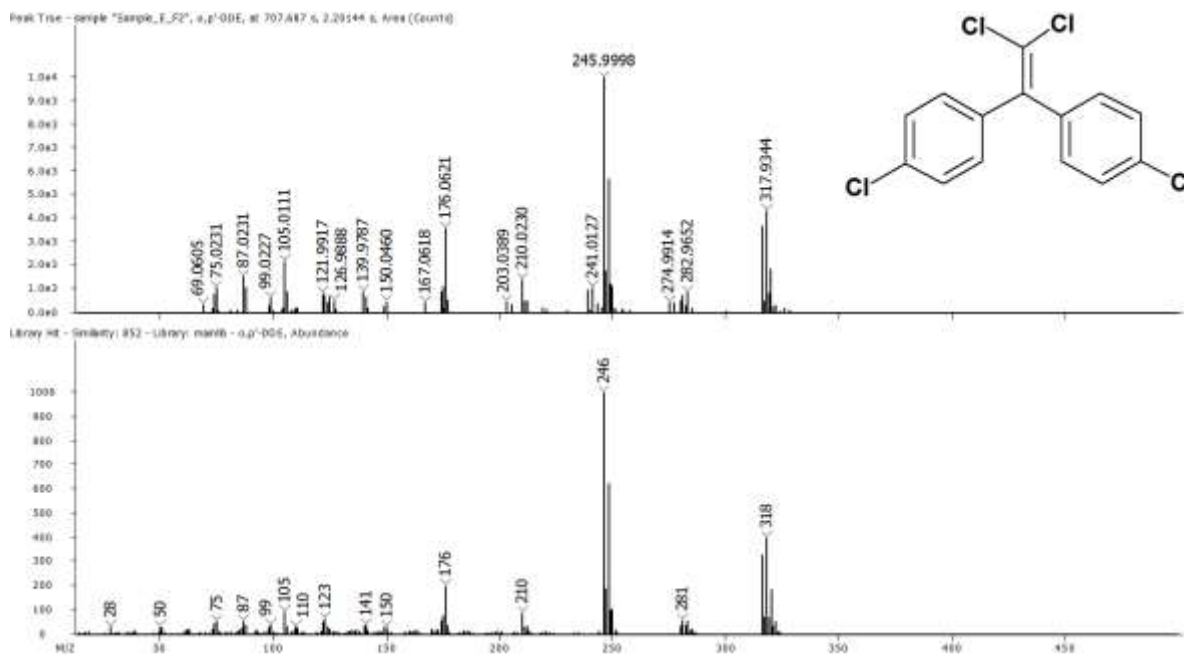


Fig. S23. 4,4'-DDE

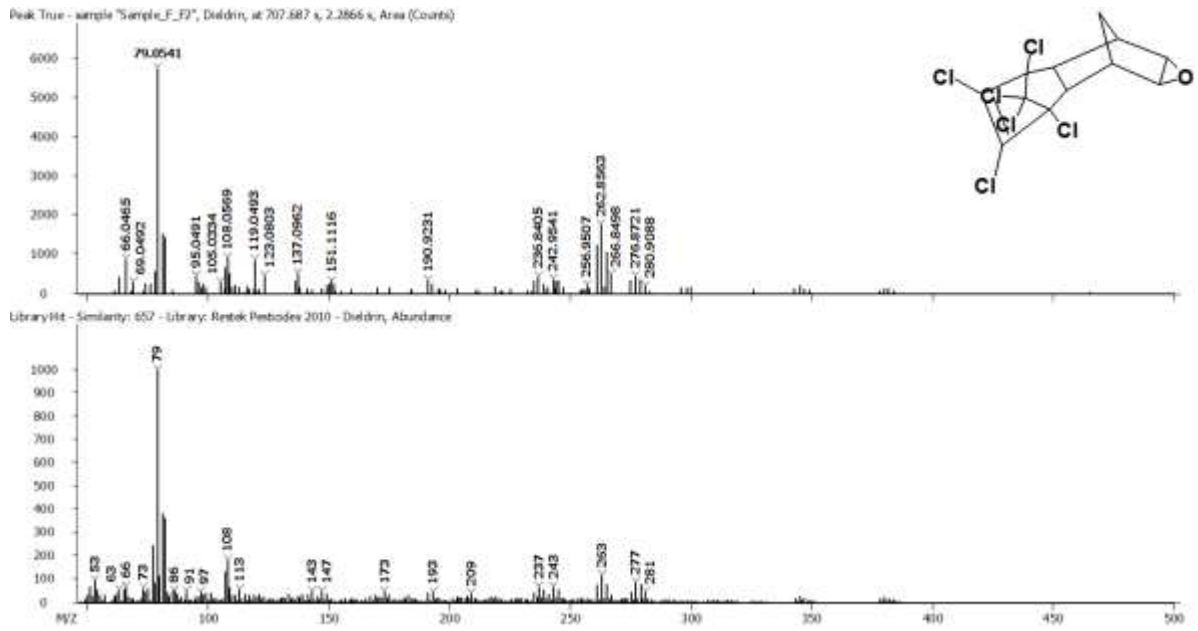


Fig. S24. Dieldrin

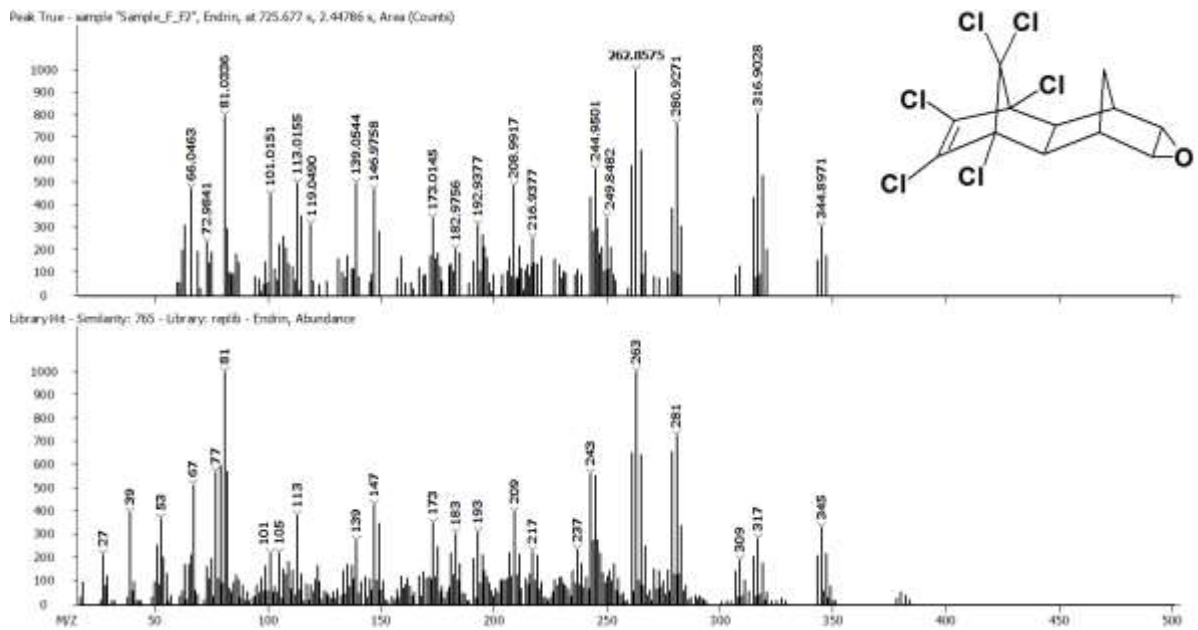


Fig. S25. Endrin

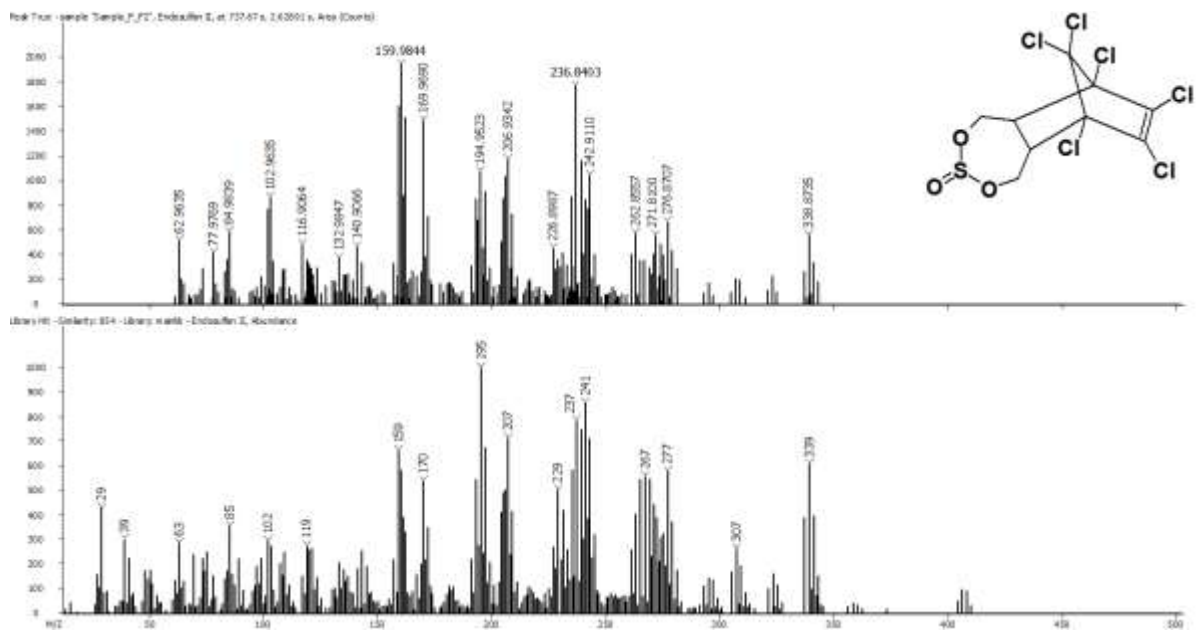


Fig. S26. Endosulfan II

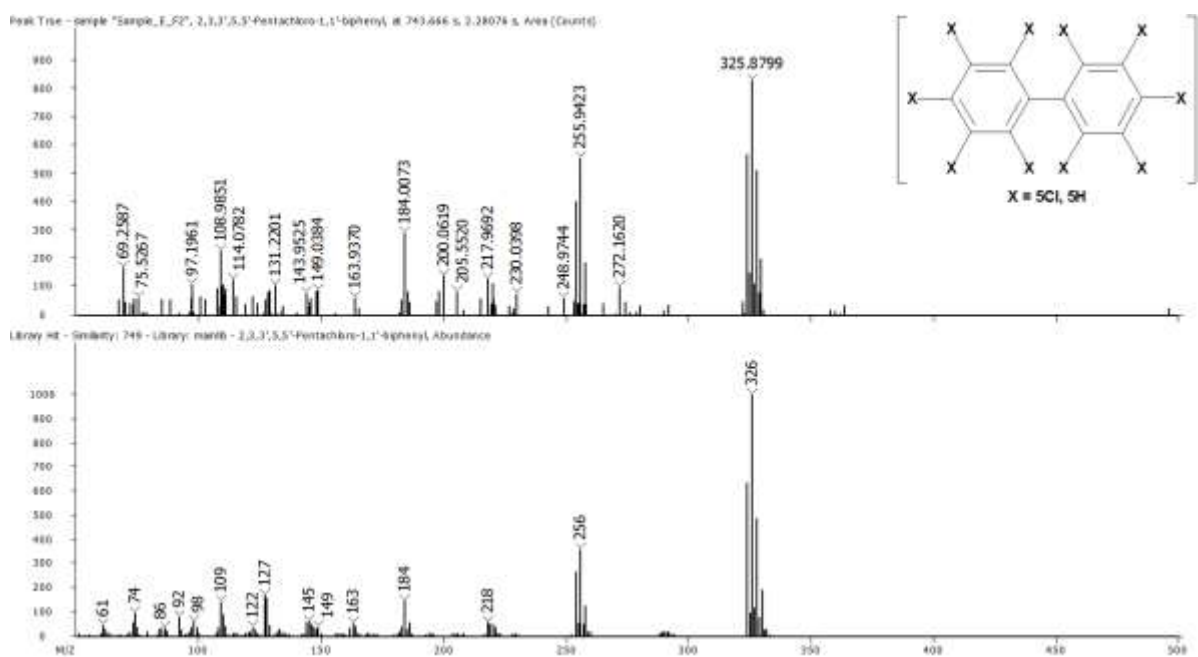


Fig. S27. Pentachlorobiphenyls (Penta-CB)

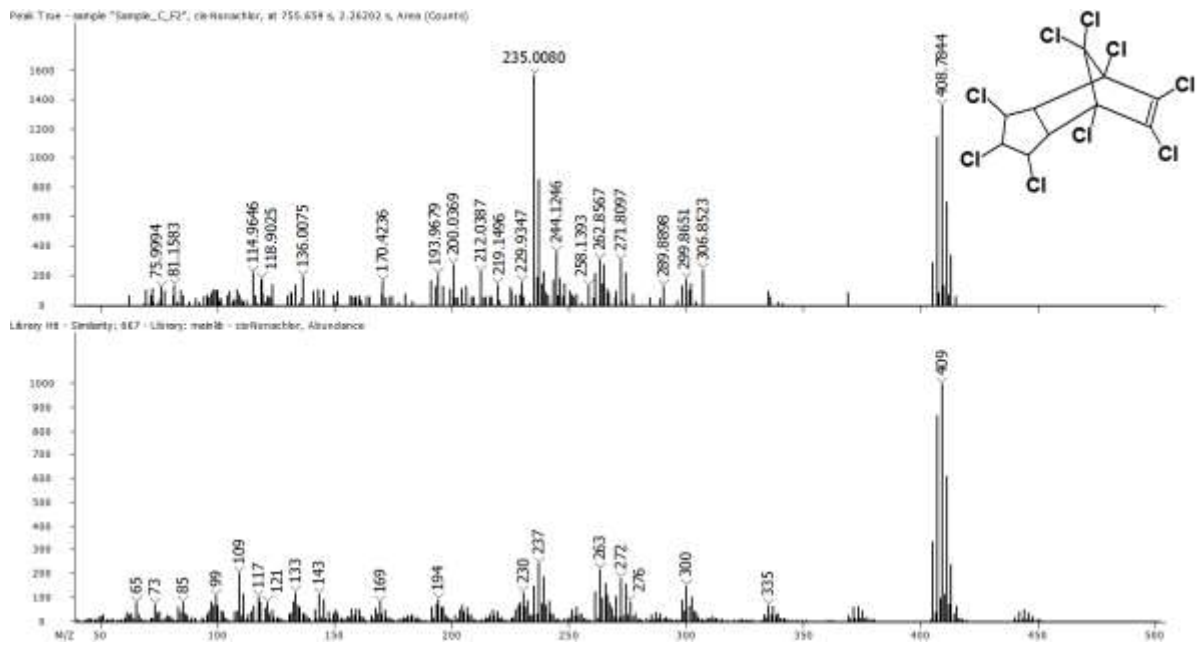


Fig. S28. cis-Nonachlor

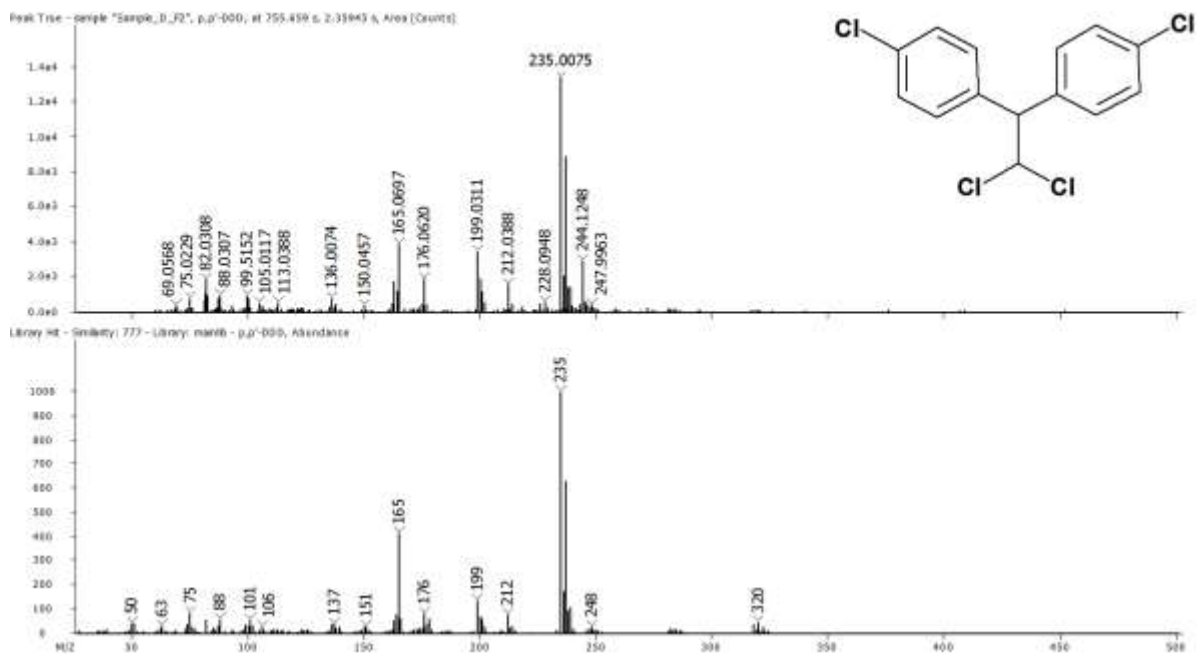


Fig. S29a. 4,4'-DDD

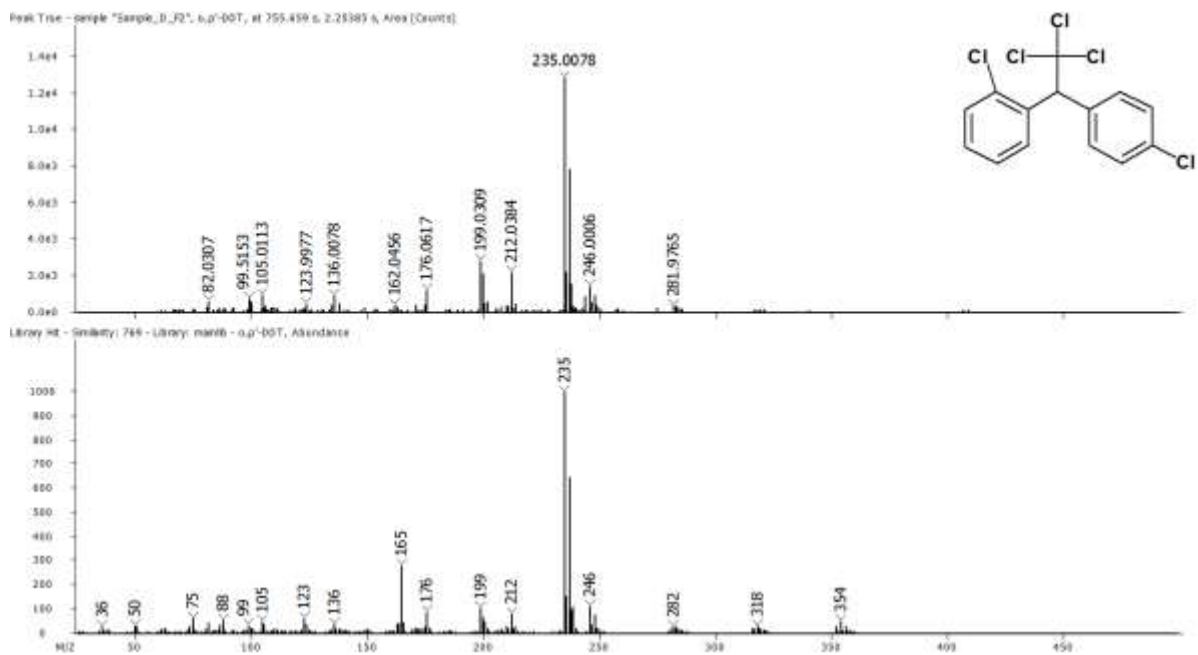


Fig. S29b. 2,4'-DDT

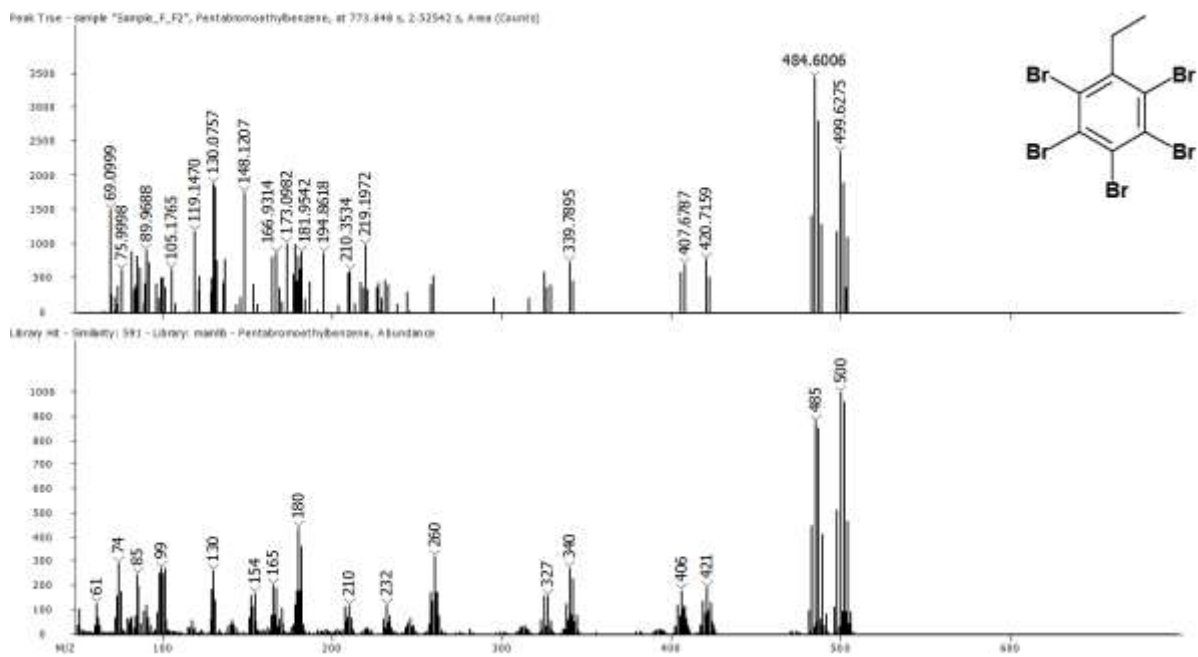


Fig. S30. Pentabromoethylbenzene (PBEB)

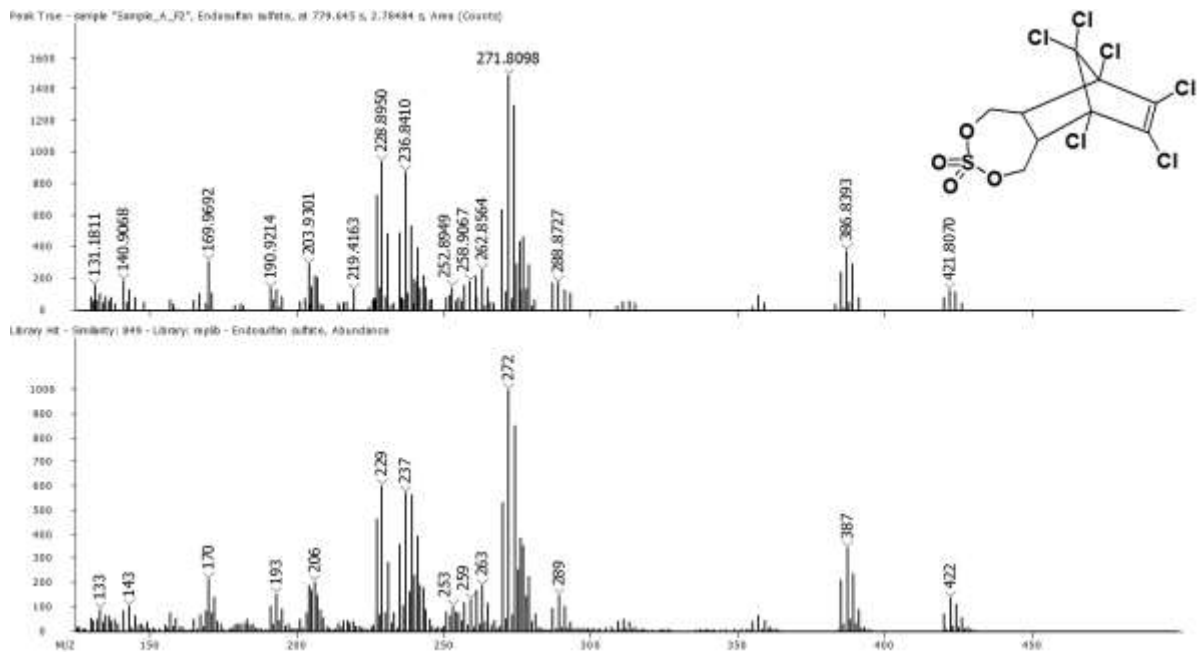


Fig. S31. Endosulfan sulfate

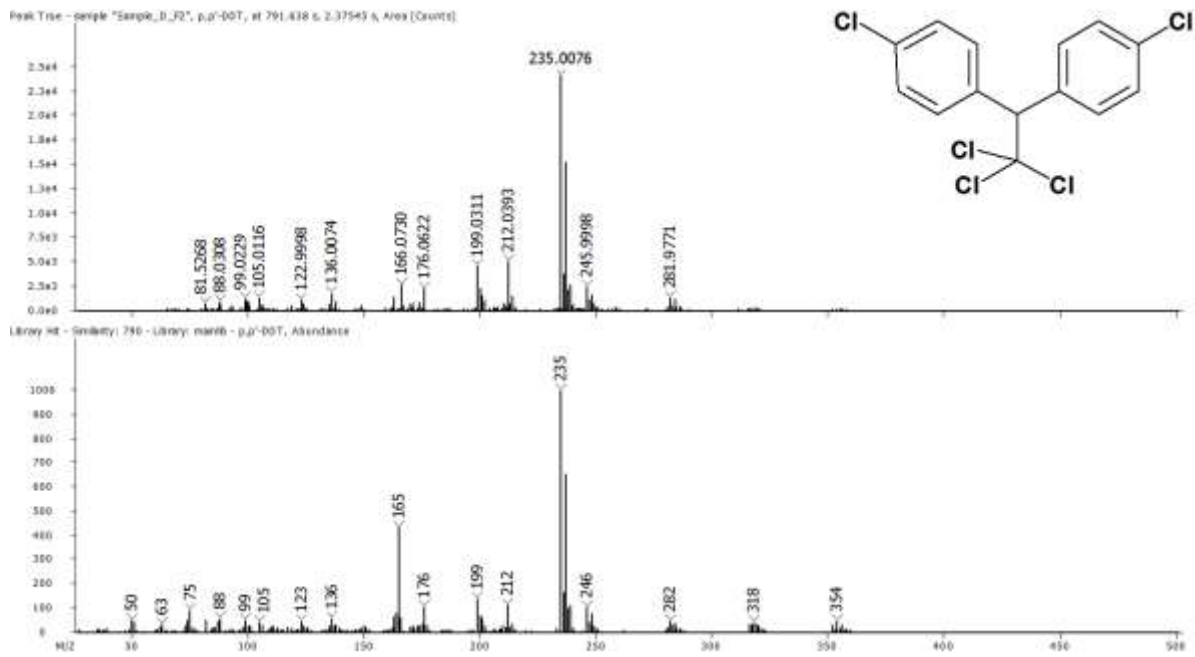


Fig. S32. 4,4'-DDT

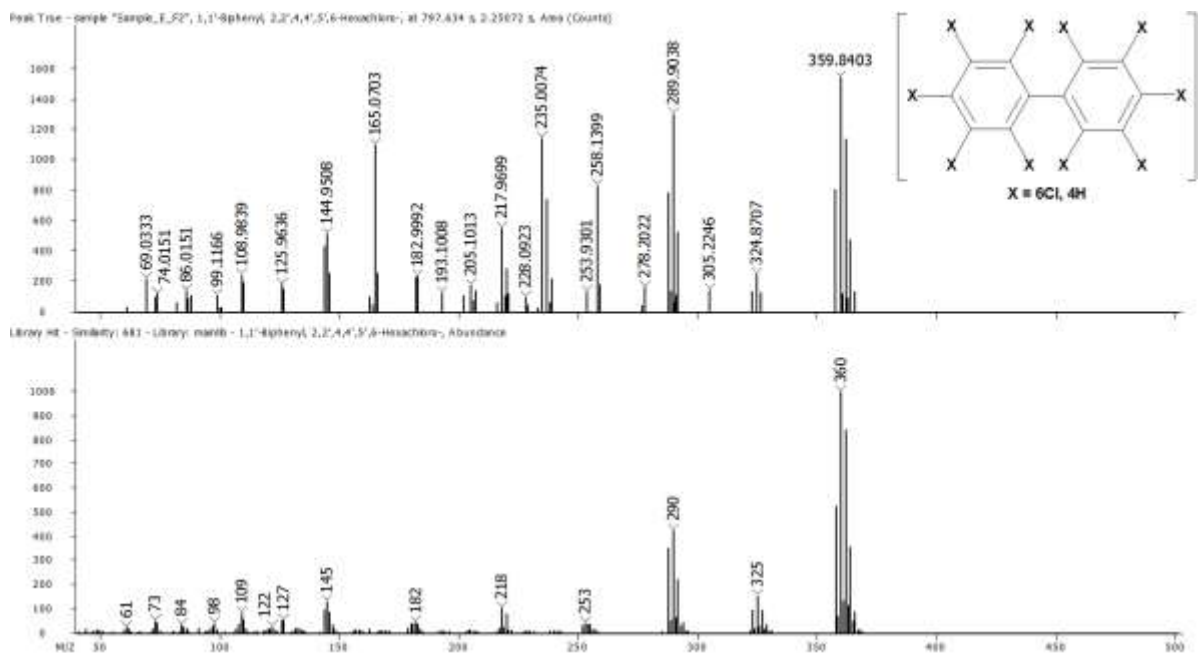


Fig. S33. Hexachlorobiphenyls (Hexa-CB)

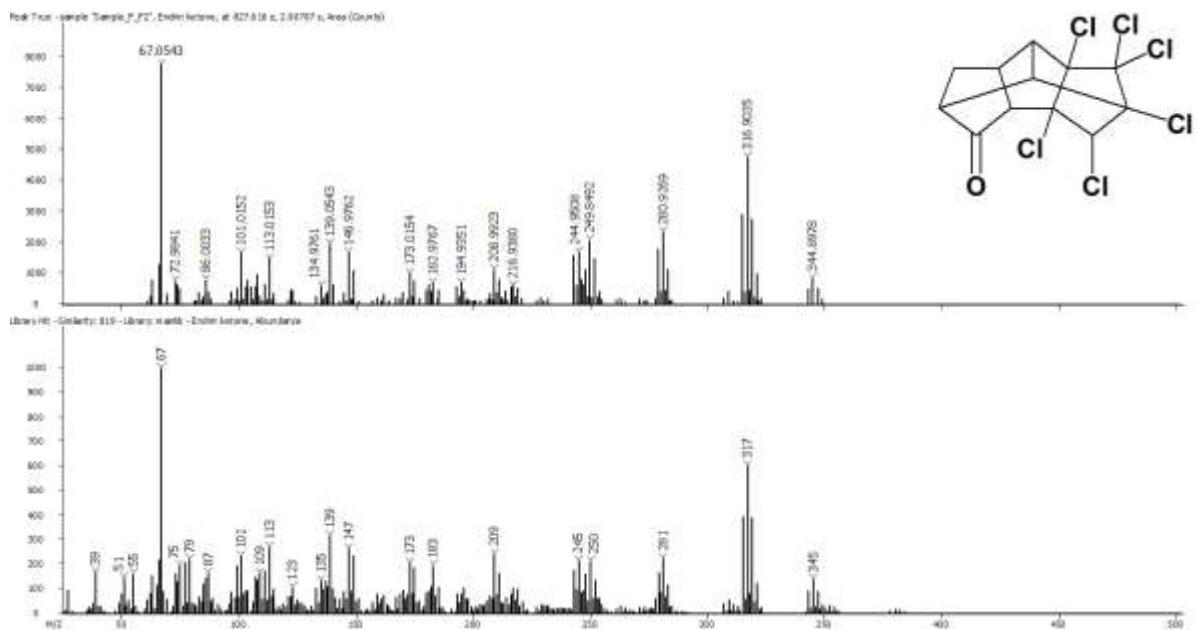


Fig. S34. Endrin ketone

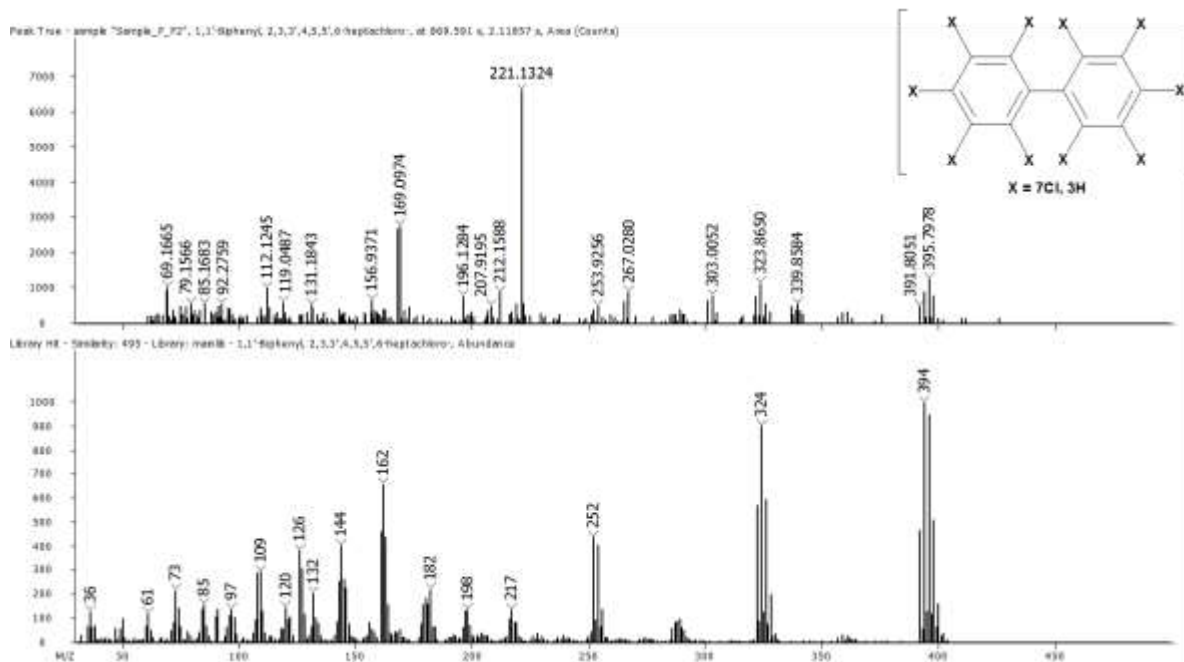


Fig. S35. Heptachlorobiphenyls (Hepta-CB)

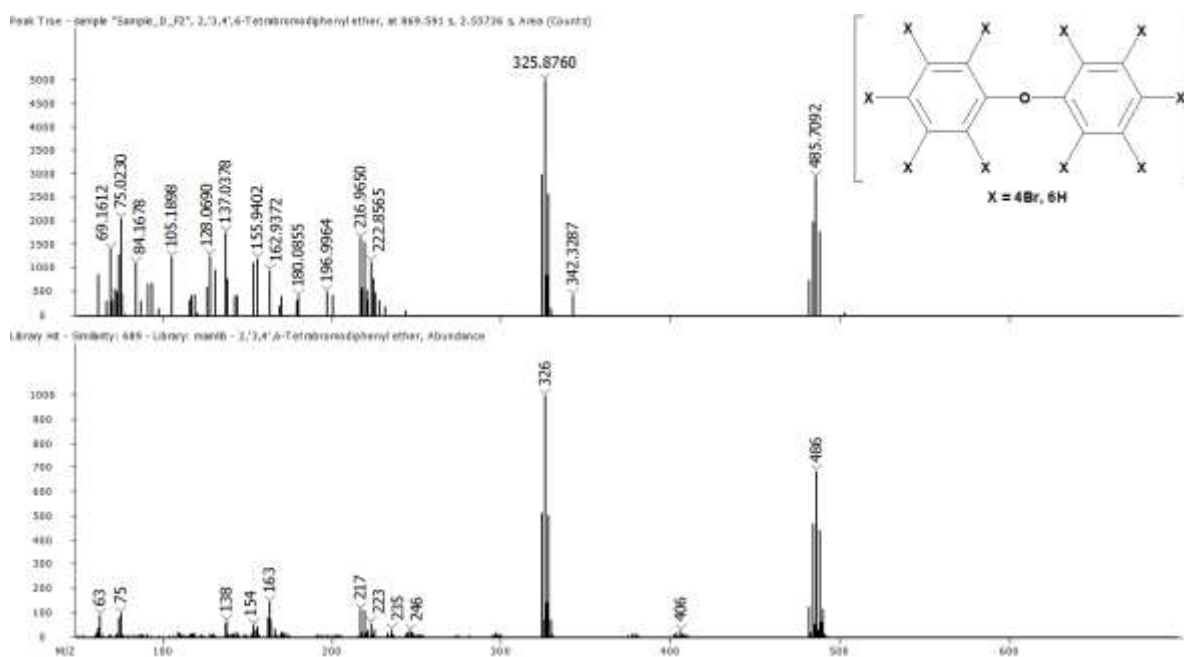


Fig. S36. Tetrabromodiphenyl ether (Tetra-BDE)

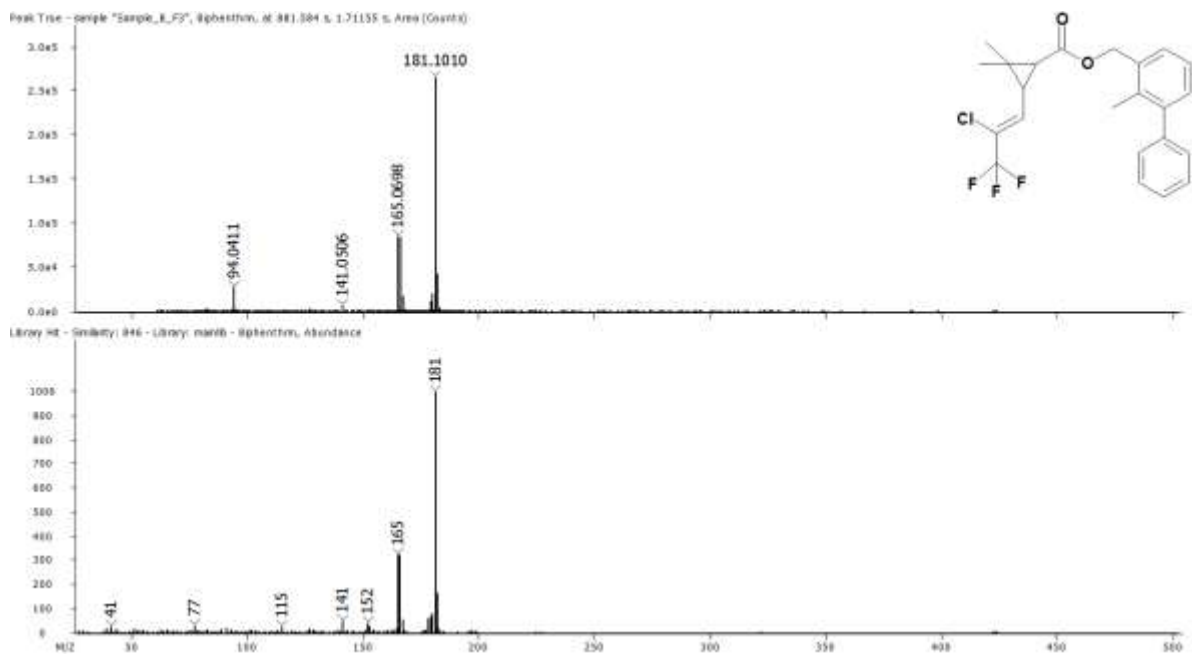


Fig. S37. Bphenanthr

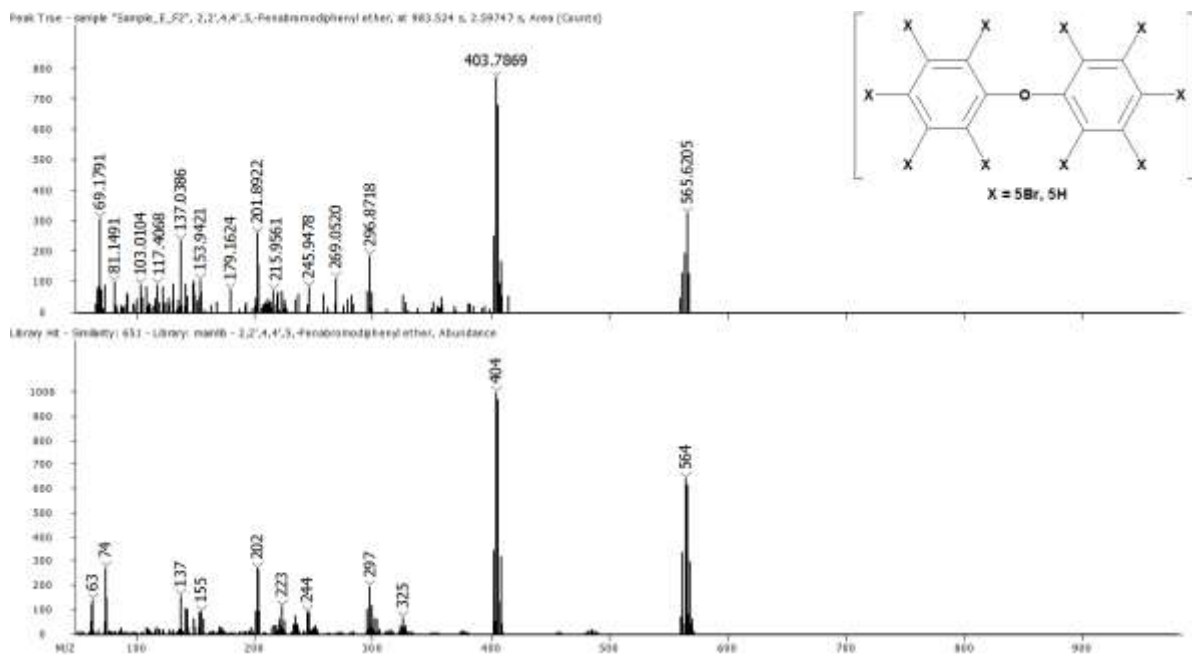


Fig. S38. Pentabromodiphenyl ether (Penta-BDE)

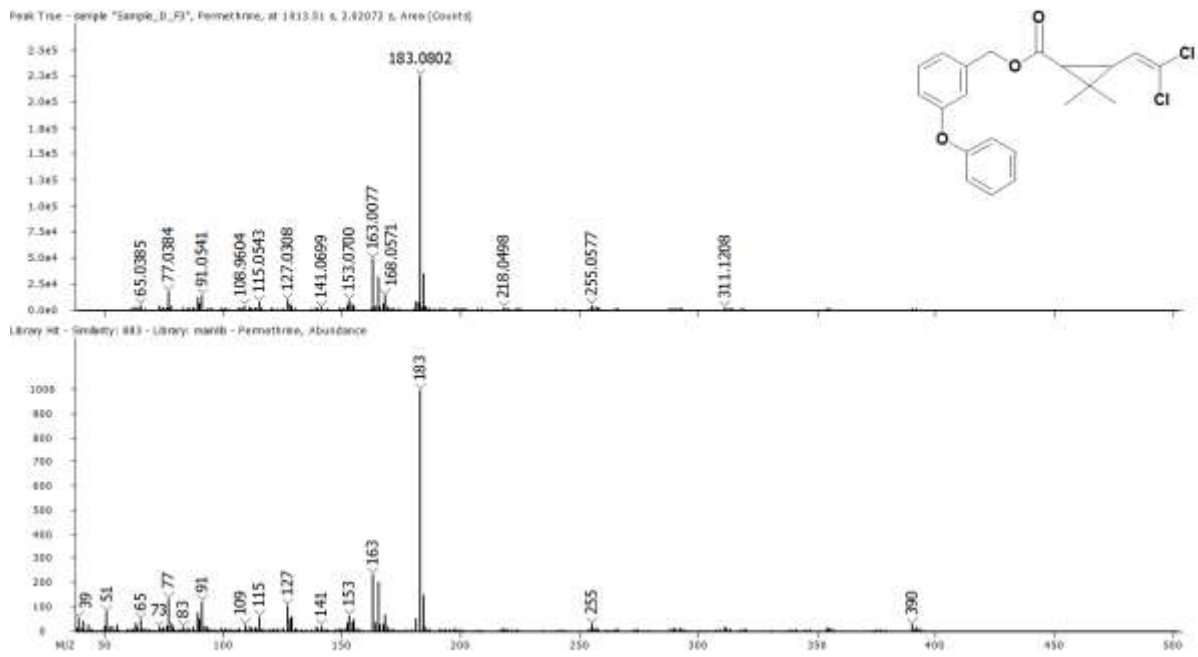


Fig. S39. Permethrin

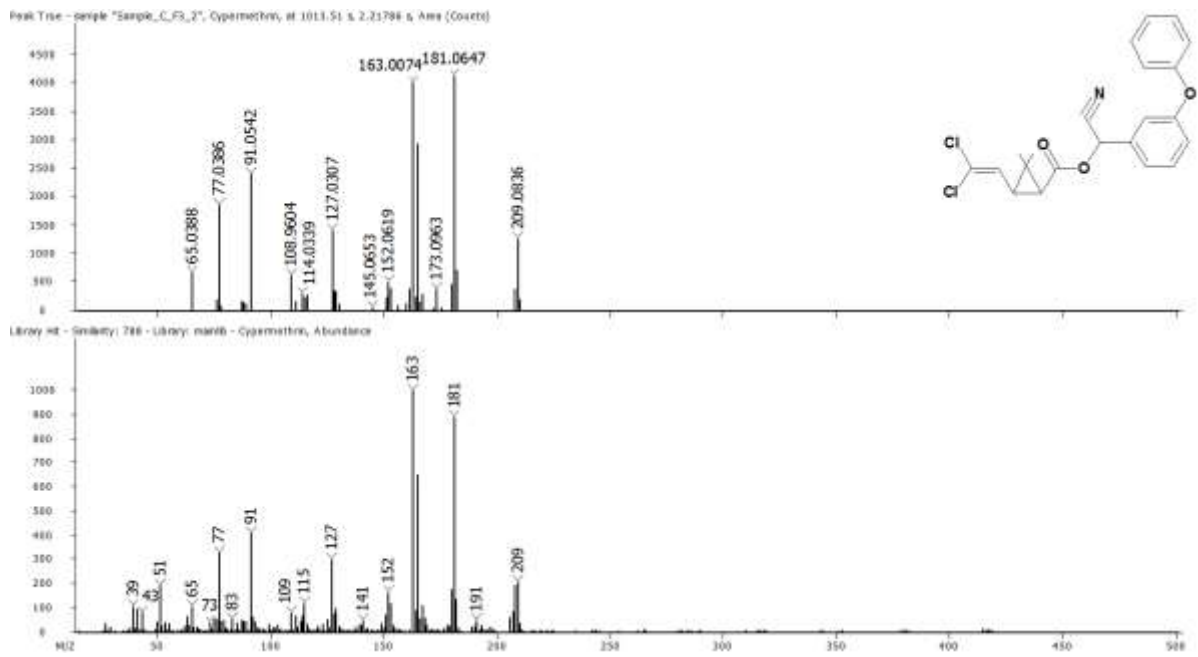


Fig. S40. Cypermethrin

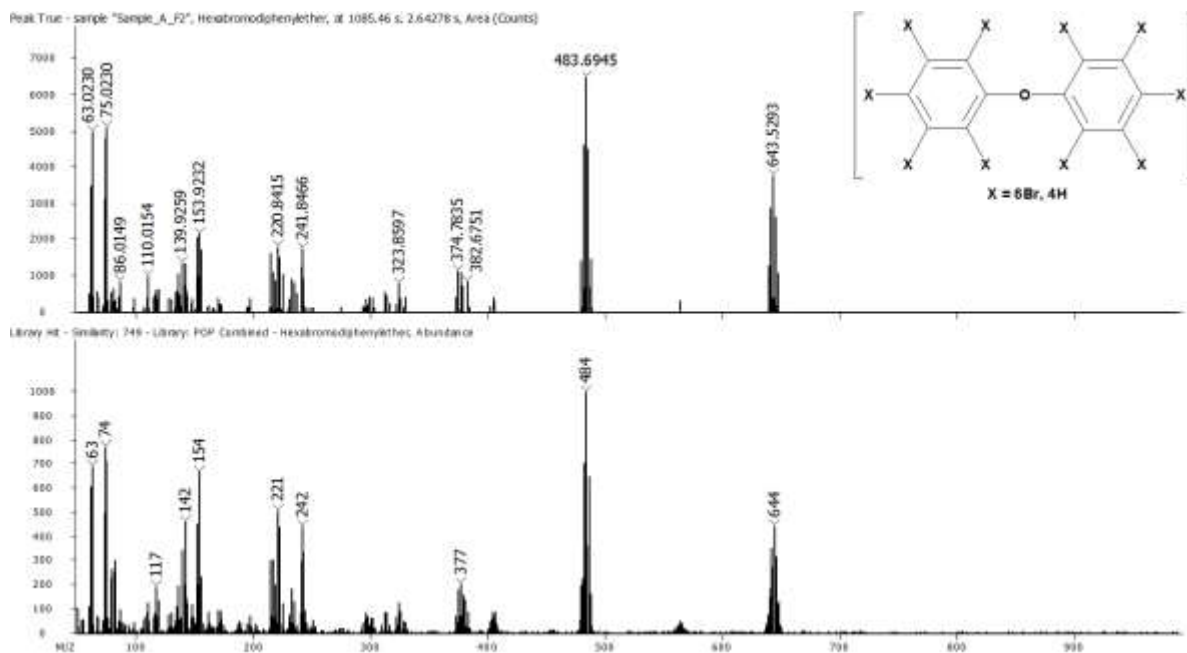


Fig. S41. Hexabromodiphenyl ether (Hexa-BDE)

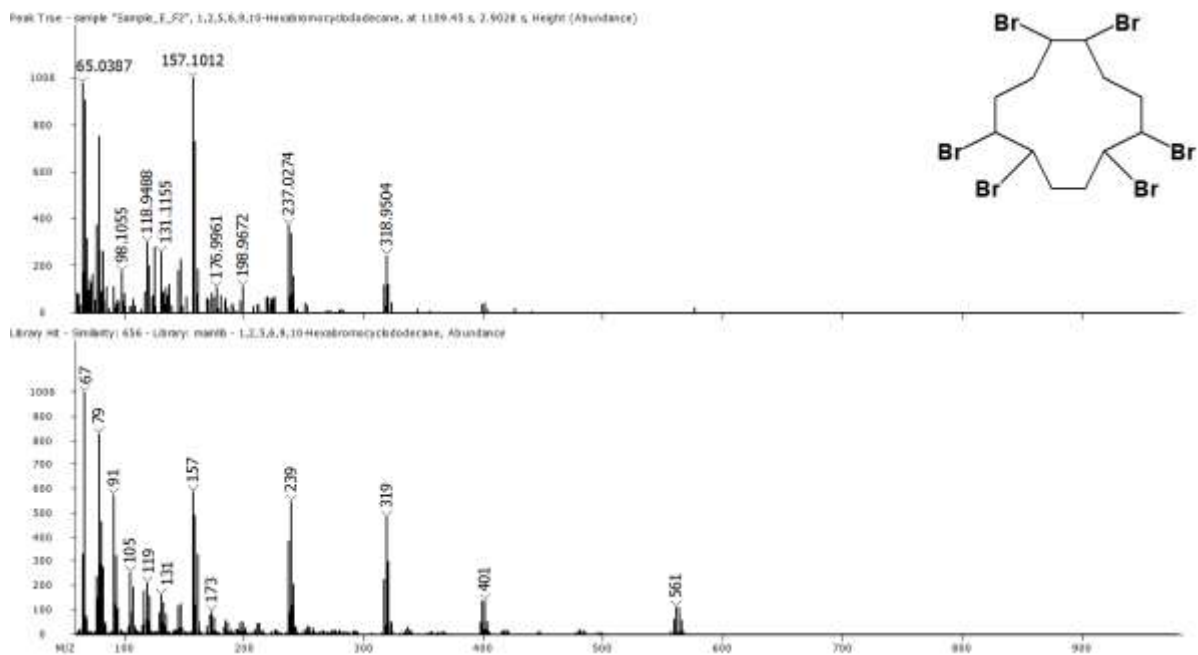


Fig. S42. Hexabromocyclododecane isomers (HBCD)

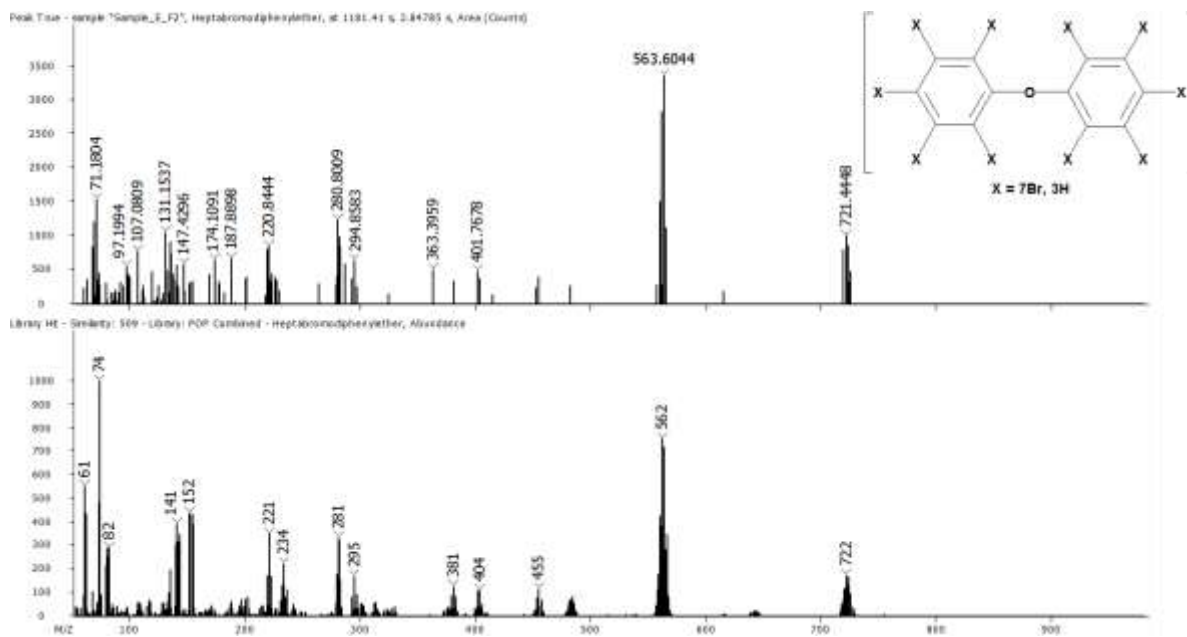


Fig. S43. Heptabromodiphenyl ether (Hepta-BDE)

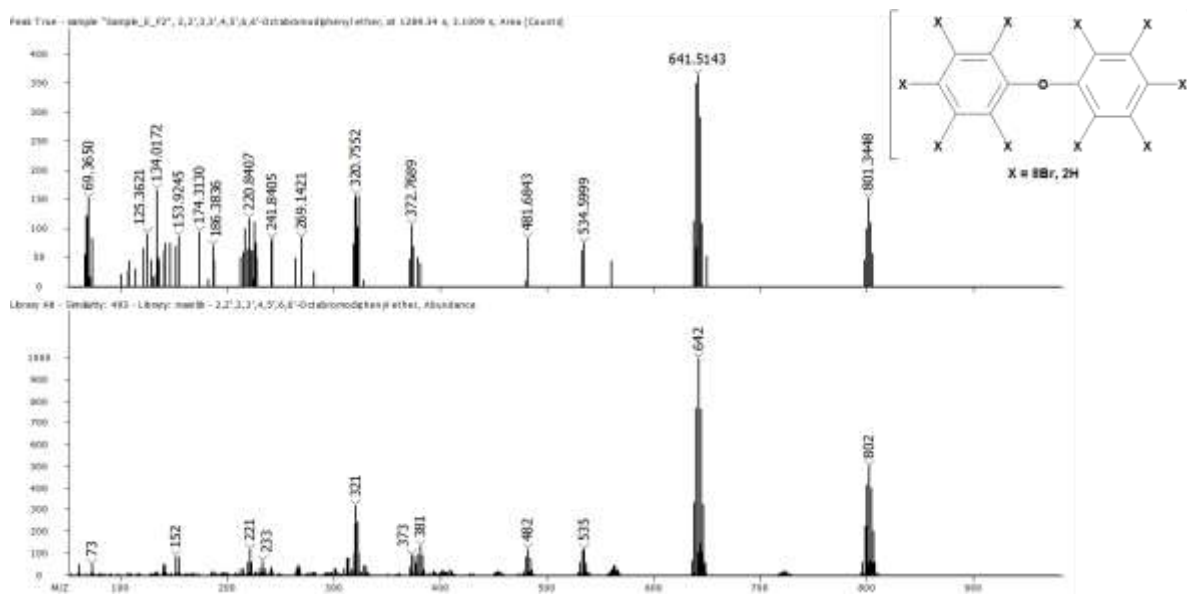


Fig. S44. Octabromodiphenyl ether (Octa-BDE)

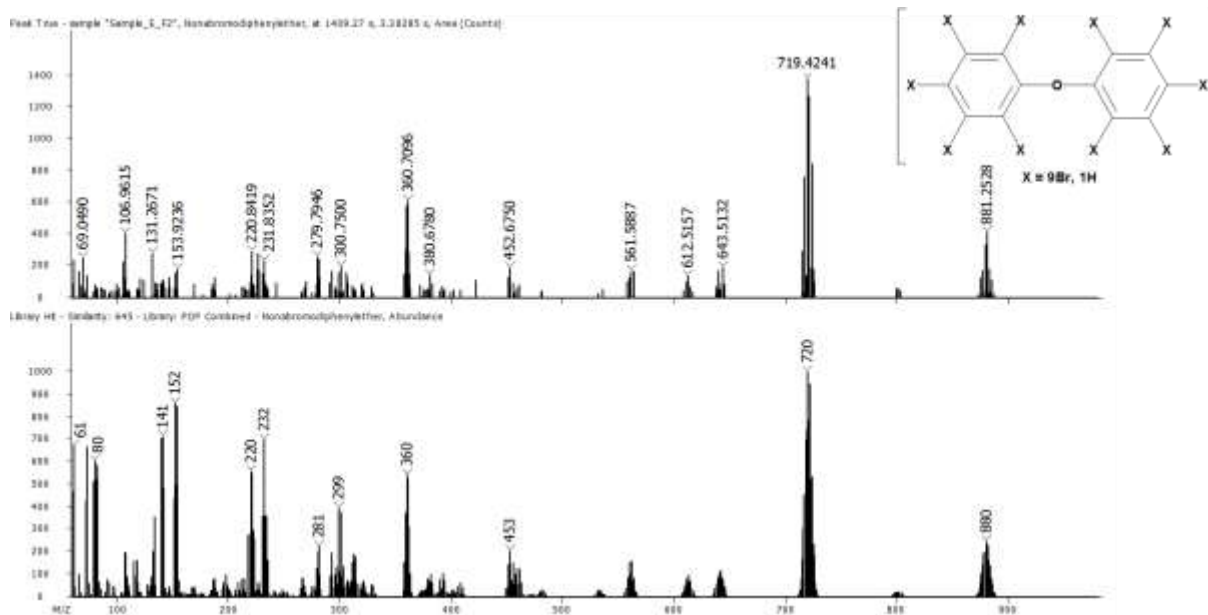


Fig. S45. Nonabromodiphenyl ether (Nona-BDE)

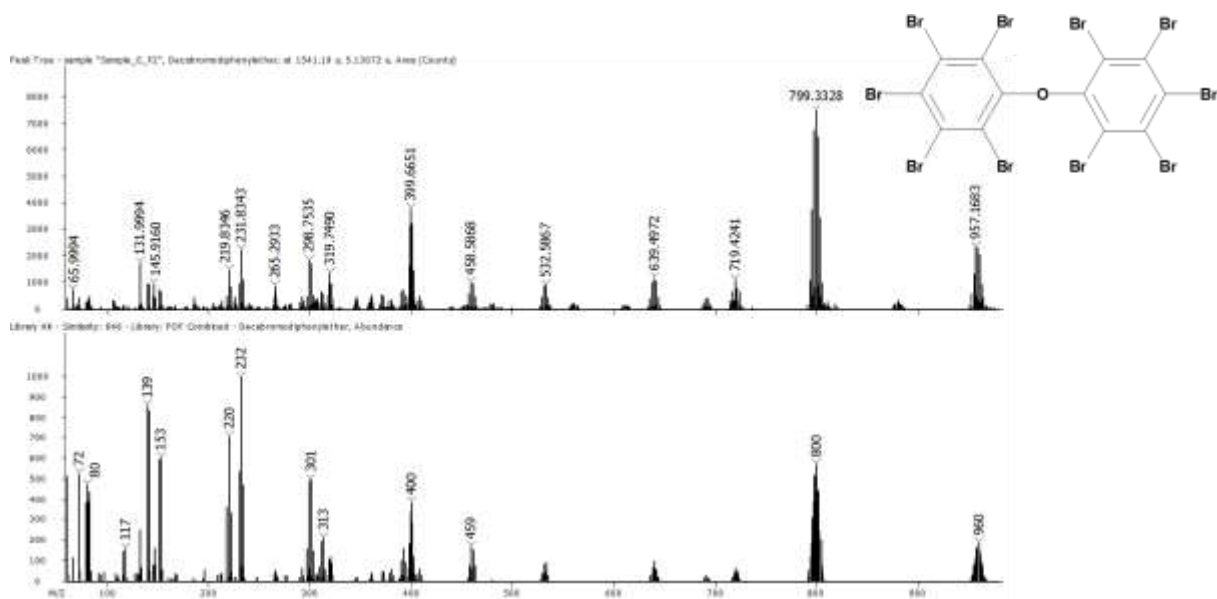


Fig. S46. Decabromodiphenyl ether (Deca-BDE)

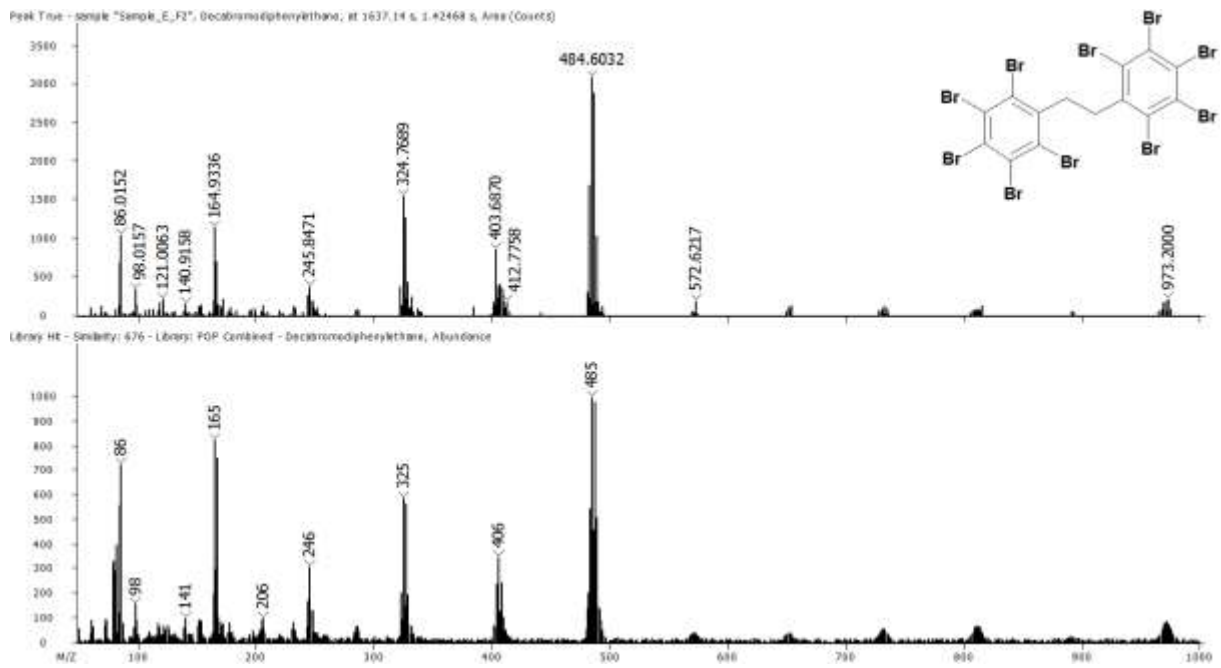


Fig. S47. Decabromodiphenyl ethane (DBDPE)